LRP 383/89 August 1989

PRECISION OF ION TEMPERATURE MEASUREMENTS IN A TOKAMAK PLASMA USING COLLECTIVE THOMSON SCATTERING: A NUMERICAL STUDY

P.A. Krug, R. Behn, S.A. Salito, M.R. Siegrist

submitted for publication in
Plasma Physics and Controlled Fusion

Precision of Ion Temperature Measurements in a Tokamak Plasma Using Collective Thomson Scattering: A numerical study

Peter A. Krug, R. Behn*, S.A. Salito*, M.R. Siegrist*

School of Physics
University of Sydney
N.S.W. 2006
Australia

* Centre de Recherche en Physique des Plasmas
Association Euratom - Confederation Suisse
Ecole Polytechnique Fédérale de Lausanne
21, Av. des Bains, CH-1007 Lausanne/Switzerland

ABSTRACT

A numerical simulation has been performed to investigate the precision of a T_i-measurement of a tokamak plasma via collective Thomson scattering at 385 μm. The study is based on a parameter and data set referring to an experiment that has been carried out at the TCA tokamak using a pulsed D_2O laser and a heterodyne receiver system. Apart from limitations due to the signal-to-noise ratio of the detection system, we investigate the influence of uncertainties in various plasma parameters required for the T_i-evaluation from a scattered spectrum. In the experiment typical relative errors of ± 25% have already been obtained, but careful optimization of the system, taking into account the results of this study, and further technical improvements should allow to reduce this limit to about ±10% for the plasma conditions considered.

1. INTRODUCTION

Recently, experiments at the TCA tokamak have succeeded in measuring the ion temperature via collective Thomson scattering from thermal density fluctuations. Using a high power pulsed D_2O laser emitting at 385μm and a heterodyne receiver comprising a Schottky diode mixer, relative uncertainties of a single shot measurement of less than 25% have been obtained[1].

It is the aim of this study to investigate the limitations in precision of such measurements and possibilities to achieve further improvements. For this purpose numerical simulations based on the parameters of the particular scattering experiment at TCA have been carried out. It will be shown that, apart from limitations in the signal-to-noise ratio determined by the parameters of the experimental setup, uncertainties in the other plasma parameters required to evaluate the ion temperature from measured spectra play an important role. This study is therefore complementary to earlier publications by Sharp et al.[2] and Watterson et al.[3], who investigated the feasibility of the method in general.

2. PARAMETER SET

For this study we have chosen a parameter set which corresponds to our scattering experiments carried out on the TCA tokamak[1]. The plasma parameters refer to ohmically heated discharges. A summary of the standard data set, which applies to all cases unless stated otherwise, is given in table 1.

3. SPECTRAL SHAPE

In the collective regime ($\alpha > 1$) the shape of the spectrum of scattered radiation depends on a number of plasma parameters in addition to T_i. Several cases are of particular interest :

- the influence of the ratio T_e / T_i
- the contributions from impurity ions
- the influence of the magnetic field

Starting from our standard data set as given in table 1, several examples are shown in Figs 1 to 3 to illustrate the characteristic changes in the shape of the spectra in these cases. We assume that there is no significant drift of the plasma parallel to the scattering wave vector $k_d = k_s - k_i$ (k_s and k_i are the scattered and incident wave vector respectively). This implies that the spectrum of scattered light is symmetrical (in frequency space), so we only need to consider one half-spectrum. It is obvious that the result of a fitting procedure which evaluates T_i from a measured spectrum will depend, sometimes rather critically, on the correct value of other plasma parameters (such as T_e, Z_{eff} etc) required as input data. Also, certain plasma conditions may be less favorable than others for a precise T_i measurement.

In particular, the cases presented in Fig. 2 show that high-Z impurity ions mainly affect the central part of the spectrum[4]. As long as there is not enough information about local impurity concentrations in the plasma, it is preferrable to exclude this central part from the analysis. Our simulation is based on the assumption that a range of spectral channels of 80MHz width are available, centered at 0, 80, 160, 240, ... MHz. The first four channels and hence signals below 280 MHz are excluded.

The effect of the angle between the magnetic field and the difference wave vector $k_d = k_s - k_i$ is shown in Fig. 3a for θ_B close to 90°. The enhancement of the scattered intensity in the centre of the spectrum is due to the magnetized electrons[5]. Averaging over the solid angle of observation reduces the effect slightly but for a cone with half angle of 2° centered at 90° it is still noticeable (see solid curve in Fig. 3a). This distortion can be avoided if the direction of observation is tilted out of the poloidal plane. Assuming that the scattering volume is near the plasma centre (as is the case in our experiment) a tilt angle of 4° is sufficient to reduce the influence of the B-field to a negligible level (Fig. 3b). θ_B can also be varied by scattering from a volume located away from the magnetic axis of the plasma, where the poloidal field component contributes to the total magnetic field.

Following these qualitative statements, we study the influence of various plasma parameters and of their uncertainties in more detail. In section 4 we investigate the sensitvity of the T_i evaluation to externally supplied plasma parameters. In section 5 the influence of uncertainties in these parameters as well as noise in the measured signals is studied. For this purpose the "real" conditions of an

experimental measurement are simulated numerically using a Monte-Carlo method.

4. INFLUENCE OF OTHER PLASMA PARAMETERS ON THE EVALUATION OF T_I

If density fluctuations at the thermal level are assumed, the spectrum of the scattered radiation for a given set of plasma parameter values can be calculated[6]. The measurement of T_i is based on a fitting procedure which compares calculated spectra with the data recorded in a number of spectral channels. By taking a calculated spectrum instead of measured data as the input to the fitting routine we reproduce the original T_{i0} value (in Figs 4 to 8 this point is identified by the intersection of the dashed horizontal and vertical lines). If, however, one of the plasma parameters supplied to the fitting routine is deliberately changed (to simulate an error in the measured value of this parameter) a different result for T_i is obtained. The amount by which this value differs from the correct one is a measure of the sensitivity of the T_i measurement to uncertainties in this particular parameter. This procedure has been applied in the following to investigate the influence of several plasma parameters on the evaluation of T_i.

4.1 EFFECT OF UNCERTAINTY IN N_E

The total scattered intensity is proportional to the number of scattering centers within the volume of observation and hence proportional to the electron density n_e. Therefore, in principle the spectral intensity could provide useful information about the plasma state. However, for a scattering experiment at submillimetre wavelengths, measurements of the absolute intensity are subject to large uncertainties. Calibration methods like Rayleigh or Raman scattering, which are employed in the visible range of the spectrum, are no longer feasible in the far infrared. Hence all parameters which influence the signal level, such as optical losses in the scattered beam path, receiver sensitivity, conversion efficiency and amplifier gain, would have to be known to a high precision to determine the absolute sensitivity of the complete system. To avoid this difficulty no attempt is made to convert the signal levels into absolute intensities. Instead, a two-parameter fitting procedure is used, one parameter being the ion temperature and the other one the scaling factor for the intensity.

The density also influences the spectra in a more subtle way, via the Debye length and the scattering parameter α. It is this influence which leads to the results presented in Fig. 4 (curve 1) showing the deviation in the evaluated T_i as a function of the supplied n_e value. From curve 1 we find that the ion temperature is overestimated by only 25% if the assumed electron density is wrong by a factor of 2. An inaccuracy of ±10% in n_e translates to a 2.25% error in fitted T_i.

The situation is much worse if fits to intensity-calibrated spectra are considered (Fig. 4, curve 2). An error in the supplied value of n_e is regarded by the fitting procedure as an incorrect value of scattered intensity. The fitting procedure attempts to produce a good fit by varying the only free variable, T_i, resulting in a very erroneous value of T_i, as shown in Fig. 4, curve 2. Incorrect ion temperatures are obtained especially when n_e is underestimated. An underestimate of only 10% in the density results in 40% error in T_i. This is the main reason why in practically all our investigations the absolute spectral intensity is ignored.

4.2 EFFECT OF UNCERTAINTY IN T_E

It has already been stated above that the ratio T_e/T_i has an important effect on the spectral shape and hence also on the precision of the measurement. Cases for various ion temperatures (300 eV, 400 eV and 500 eV) have been studied and the results are presented in Fig. 5. We find that the larger the ratio T_e/T_i, the smaller are the errors in T_i for incorrect T_e - values. For T_{i0} = 400eV a 10% error in T_e results in over 15% error in T_i. For this reason it is essential to have an accurate independent T_e diagnostic available. Underestimating T_e leads to smaller errors in T_i than overestimating it.

The spectrum of a deuterium plasma, with the standard parameter values given in table 1, does not show a pronounced ion-acoustic feature. This is quite different for a helium plasma with similar parameters where the ion acoustic resonance is well developed due to the higher mass and charge of the ions. We show in the same Fig. 5 the sensitivity of a T_i measurement to variations in T_e for a He-plasma with otherwise identical parameters to our standard D-plasma. It is clearly far less sensitive to uncertainties in T_e.

4.3 EFFECT OF UNCERTAINTY IN B

As has been mentioned earlier the electron gyration enforced by the magnetic field leads to changes in the spectra also in the case of collective scattering. Since this effect depends strongly on the orientation of the difference wave vector k_d to the total magnetic field B , we expect that errors in the value of the angle θ_B supplied to the fitting routine will lead to significant errors in the evaluation of T_i. Fig. 6 shows this dependence for two cases : θ_B = 88°, which corresponds to the observation of a scattering volume near the plasma centre along a direction in the poloidal plane; and for θ_B = 86°, which refers to the conditions of the latest experiments on TCA[1].

Since the influence of the magnetic field is only important for θ_B near 90°, the errors do not further increase for angles supplied to the fitting routine below 70°. For the case of θ_B = 86° an error of not more than 20% is incurred if the influence of the magnetic field is neglected completely, whereas at θ_B=88° the temperature would be overestimated by 75%.

For a given angle the field magnitude is far less critical. This is shown in Fig. 7 for our standard conditions. A 10% error in the field value results in only 4.4% uncertainty in T_i.

4.4 EFFECT OF UNCERTAINTY IN Z_{EFF}

The sensitivity of the T_i-measurement to uncertainties in Z_{eff} is shown in Fig. 8. For the three cases presented here different species of impurity ions have been included (curve 1 : mixture of C, O, and Fe; curve 2 : C and O; curve 3 : Fe only). The concentrations have been adjusted to obtain the same true Z_{eff} of 2.53 in all cases. When Z_{eff} is changed to study its influence on the Ti-evaluation, the concentrations of all impurity species are varied in proportion. In accordance with the standard parameter set the central part of the spectrum (ν < 280 MHz) has been excluded. This explains why in the case with a heavy impurity only (curve 3) the influence of Z_{eff} is rather small. However, the presence of light impurities can lead to large errors in a T_i measurement especially if their concentrations are underestimated.

5. NUMERICAL SIMULATION OF A SCATTERING EXPERIMENT

So far we have studied the influence of uncertainties or errors in various plasma parameters by deliberately changing the data fed into the fitting routine. Instead of experimental data, calculated spectra were used which did not contain any statistical fluctuations. In the following the real conditions of a scattering experiment are simulated numerically[3]. Using a Monte-Carlo technique random noise is added to the calculated spectra. The noise level is expressed in terms of an NEP (noise equivalent power referred to the receiver input) and comprises the influence of fluctuations in the background radiation and the contributions from detector and amplifier noise. In the case of a heterodyne receiver with bandwidth of each spectral channel dv and an integration time τ the signal-to-noise ratio is expressed by equ. (1) :

$$(1) \qquad \frac{S}{N} = \frac{P_S}{(P_S + P_n)} * \sqrt{1 + dv \cdot \tau,}$$

where P_S is the power of the scattered radiation collected by the receiver and P_n represents the power equivalent to the noise. A sample spectrum $P_s(\omega_i)$ is obtained from i = 1, ..., N theoretical values $P_t(\omega_i)$ by :

$$(2) \qquad P_s(\omega_i) = \chi_m^2 \, [P_t(\omega_i) + P_n(\omega_i)] - P_n(\omega_i)$$

with a χ^2-distribution of $m=2(dv\,\tau + 1)$ degrees of freedom[3]. Each simulation consists of a series of sample spectra (in our case 31). From a fitting procedure we obtain a set of T_i values which represent possible results of a measurement for the given conditions.

The numerical simulation also permits us to investigate by statistical means the influence of uncertainties associated with measured plasma parameters that have to be supplied to the fitting routine. For each sample spectrum the value of each important plasma parameter is taken at random from a Gaussian distribution which is centered at the measured value of the particular parameter. The width of this distribution (usually expressed as fractional variation in the parameter) is related to the uncertainty of the measurement from which this parameter has been obtained. The statistical analysis of the set of T_i values allows determination of the accuracy of the T_i evaluation and reveals systematic deviations.

5.1 THE QUALITY OF THE FIT

For the fitting procedure we define as merit function $F(T_i)$ the RMS value, summed over all spectral channels, of the differences between the artifically created noisy spectrum and the theoretical spectrum which corresponds to the particular T_i found by the fitting routine. It is in fact this quantity that is minimized during the fitting procedure. Therefore, the smaller $F(T_i)$ the better the fit. Also, in order to obtain meaningful results, $F(T_i)$ should have a pronounced minimum. If the minimum is rather shallow we cannot expect to resolve small changes in T_i. Such a situation can occur when either the spectrum does not change significantly with ion temperature or the signal-to-noise ratio is too small.

Figure 9a shows $F(T_i)$ versus T_i for an ideal, noiseless case where all the parameters are exactly and correctly known. It is evident that the curve has a very pronounced minimum (0 to within numerical precision in this case) at exactly 400 eV (the true T_i value). In Figure 9b the five curves plotted differ from Fig. 9a (and each other) due to the presence of noise in the "experimental" spectrum. The curves, corresponding to five separate "shots", all show a clear minimum, albeit much less pronounced than in the noiseless case. The estimated Ti values are also no longer exactly 400 eV.

If we assume uncertainties in n_e, T_e and B at the same time we obtain the results presented in Fig. 9c . Some of the shots show F(Ti) with either a broad, poorly defined minimum in the vicinity of 1000eV (shot 5), or else decreasing to some minimum value well beyond the plotted range (shot 1).

The curve $F(T_i)$ is clearly asymmetric. This reflects the fact that variations in the spectral shape are much more pronounced for small T_i values. Hence it is less likely that the evaluated T_i will be too low, whereas a spectrum with a large T_i might still produce a reasonably good fit.

5.2 EFFECTS OF UNCERTAINTIES IN OTHER PLASMA PARAMETERS

In addition to the statistical fluctuations caused by noise we can also assume uncertainties (expressed as a fractional variation) in one or several of the externally supplied plasma parameters. In Fig. 10 we show the result of simulation runs for specified fractional variations in T_e. In Fig. 10a the standard deviation of

T_i-fits (S) is expressed as percentage value of the true ion temperature and Fig. 10b shows the difference between the mean of the fits and the true T_i-value (E), also expressed as percentage of the true value. For the data set of table I, and with all plasma parameters precisely known, the mean systematic error in T_i is ± 3% with a shot to shot scatter of 17 ± 3%. As the fractional variation in T_e is increased from zero to 0.2 or more, the mean systematic error rises to about 9% of T_{i0}, and the shot-to-shot scatter to over 35%. If, however, T_e can be reliably mesured to within 10% of the true value, the values of E and S remain small. Figure 11 shows the relationship between T_e supplied to the fitting routine and T_i estimates. It confirms the behaviour observed with noiseless spectra (Fig. 5, curve labeled 400 eV).

For the investigation of the influence of uncertainties in the impurity contents a single variable, ΔF_i, determines the statistical scatter in the supplied abundances of all three impurity ions. In Fig. 12 E and S are plotted against ΔF_i. For each shot the abundances of the three impurity species are independent of each other. Since they vary randomly and independently, we plot in Fig. 13 estimated T_i against the fractional abundance of the deuterium ion. To account for uncertainties in the other plasma parameters we assume $\Delta n_e = 0.05$, $\Delta T_e = 0.10$ and $\Delta B = 0.03$. Figures 12 and 13 show only a slight dependence of estimated T_i on impurity abundance. The mean systematic error in T_i remains constant at about 5±5% for ΔF_i up to 0.8, and the shot-to-shot scatter rises from about 22% to 30% as ΔF_i ranges from 0 to 0.8.

According to the results presented in Fig. 8, the T_i-values obtained are too large if the impurity concentration is underestimated (fractional abundance of deuterium ions > 0.968) and vice versa. This is also observed in Fig. 13. The results of Figures 12 and 13 represent a case where the concentrations of all impurities have been measured independently (with limited precision). In reality often Z_{eff} only is measured (sometimes only estimated). Under these circumstances systematic effects like the peak around Z_{eff}=1.5 in Fig. 8 are more important.

The measurement precision depends strongly on the shape of the spectrum. In the case of $T_e / T_i >> 1$ the spectrum (Fig. 1) shows a pronounced ion-acoustic resonance. Its width and position are very sensitive to a change in T_i at fixed T_e. Therefore a more precise T_i measurement should be obtained at low T_i where the ratio of T_e / T_i is large. This is demonstrated with simulation results in Fig. 14. As function of the ion temperature, for fixed electron temperature of 700eV, we show

the standard deviation of 31 T_i values with respect to a single measurement expressed as percentage of the true value. Two sets of simulation runs were done for each T_i value assuming that all other plasma parameters are known exactly. The shot-to-shot scatter of 5% for small T_i increases to 20% for plasmas with $T_e=T_i$.

5.3 EFFECT OF THE RECEIVER SENSITIVITY AND POSITION OF THE SPECTRAL CHANNELS

Up till now we have discussed the influence of imprecisely known plasma parameters on the precision of an ion temperature measurement with collective Thomson scattering. If these parameters were all accurately known, the measurement precision would be limited by the signal-to-noise ratio. According to equation 1 the S/N ratio achievable is finally limited by the square-root term since $P_s/(P_s+P_n)$ can never exeed one. The maximum value possible for the system discussed (80MHz channels, 1.38μs integration time) is 10.5.

In Fig. 15 we show the spectrum for our standard conditions (solid line), the signals in each channel obtained from a particular simulation run (circles) and the standard deviations σ of 31 simulations, represented as error bars of length 2 σ, centered on the means. A similar graph would be obtained from a real scattering experiment. The S/N ratios range from approx. 7 to 10 and hence are very close to the theoretical limit. Experimentally signal to noise ratios of only half of these values have been achieved so far[1]. S/N ratios of 8 and 4 translate into pre-integration signal-to-noise ratios of 3.2 and 0.6 respectively. The precision or shot-to-shot scatter achievable in the case of exact plasma parameters is degraded by approximately 50% in going from the standard NEP of $5*10^{-19}$W/Hz to $2.5*10^{-18}$W/Hz (Fig. 16). Hence further efforts to either increase the detection sensitivity by up to a factor of 5 (possible with state-of-the-art Schottky diode mixers) or the power delivered by the laser (difficult to achieve) would be worthwhile. Also, losses in the optical system should be further reduced.

Optimization of the instrumental parameters should also deal with the position of the receiver channels with respect to the spectrum to be observed. In the following we assume that the number of channels and hence the total covered bandwidth are fixed but their position relative to the spectrum can be changed. We have already mentioned that the inclusion of the line center is not advisable since parasitic stray light, scattering from impurities and contributions from non-thermal fluctuations all influence the signal close to line center. On the

other hand, if the spectral band is too far out in the wings of the thermal feature, poor signal-to-noise ratio precludes an accurate fit. Obviously there must be an optimum between these extremes.

For the following simulation runs (Fig. 17) it has been assumed that $\Delta n_e=0.05$, $\Delta T_e=0.10$ and $\Delta B=0.03$. It is also assumed that the total spectral band covered is 960MHz, consistent with the 12 channels of 80MHz bandwidth each as given in table I. The precision is of the order of 25% for cutoff frequencies up to 360 MHz. It then drops to below 10% where it remains up to a cutoff frequency as high as 1080 MHz. Thereafter it rises rapidly. From these results we conclude that it is advantageous to include receiver channels near the wings of the spectrum, even if the scattered intensity is low. Such an arrangement reacts in a more sensitive way to changes in T_i. The signals in the central channels are higher, permitting better signal-to-noise ratios, but their relative variation with T_i is smaller.

6. CONCLUSIONS

Using numerical simulations we have investigated the precision of an ion temperature measurement of a tokamak plasma by collective Thomson scattering from thermal density fluctuations. The parameters used during this study refer to experiments carried out at the TCA tokamak. They are typical for a scattering experiment using a pulsed D_2O laser at 385 μm and a heterodyne receiver comprising a Schottky barrier diode mixer. Therefore the case studied here may serve as an example which points out some important aspects that have to be taken into account when designing a collective scattering experiment to measure T_i . In particular, we have shown that it is essential to know other plasma parameters (especially T_e) with sufficient precision. Care should be taken when selecting the distribution of the spectral channels of the receiver system in order to obtain optimum sensitivity to variations in T_i.

The quoted precision of a T_i-measurement depends on the parameters of the tokamak plasma and the specifications of the experimental set-up. Although they can be regarded as typical, a careful reevaluation will be necessary for other cases taking into account the specific conditions which may be different from those considered in this study. As far as our experiment on TCA is concerned, further improvements still seem to be possible (e.g. improving the receiver sensitivity, rearranging the spectral channels). In this way the relative

uncertainty of a T_i measurement could be reduced to about 10% under optimum conditions.

In the future, other coherent radiation sources (e.g. gyrotrons or FELs) allowing longer pulses and integration times may become available. In this case, either a substantial improvement in the signal-to-noise ratio can be obtained or measurements at lower plasma densities become feasible.

ACKNOWLEDGEMENTS

This work has been supported by the Ecole Polytechnique Fédérale de Lausanne, the Swiss National Science Foundation and EURATOM.
P.A. Krug acknowledges an Australian National Research Fellowship Queen Elizabeth II Fellowship, and associated Research Support Grant.
We thank the University of Sydney and the Science Foundation for Physics for provision of facilities.

REFERENCES :

1 R.Behn, D.Dicken, J.Hackmann, S.A.Salito, M.R.Siegrist, P.A.Krug, I.Kjelberg, B.Duval, B.Joye, A.Pochelon,
Phys. Rev. Lett. 62, 2833-2836 (1989)

2 L.E.Sharp, A.D.Sanderson, D.E.Evans,
Plasma Physics 23, 357-370 (1981)

3 R.L.Watterson, M.R.Siegrist, M.A.Dupertuis, P.D.Morgan, M.R.Green,
J.Appl.Phys. 52, 3249-3254 (1981)

4 D.E.Evans,
Plasma Physics 12, 573-584, (1970)

5 T.J.M.Boyd, D.E.Evans, G.A.Gardner,
Proc. 10th Int. Conf. on Phenomena in Ionized Gases,
Parsons, Oxford, p. 412

6 M.R.Siegrist, M.A.Dupertuis, R.Behn, P.D.Morgan,
Plasma Physics 24, 1449-1463 (1982)

FIGURE CAPTIONS

Fig. 1: Spectra for the standard conditions defined in table I and variable T_i. For fixed T_e=700eV the ratio T_i/T_e is 0.1, 0.2, 0.5, 1, 2, 5, 10 for the curves 1 to 7.

Fig. 2: Spectra for standard conditions and no impurities (curve 1), light impurities (C, O, curve 2), the heavy impurity Fe (curve 3) and the standard impurity composition according to table I (curve 4). The impurity concentrations have been adjusted in proportion to give Z_{eff}=2.53 (curves 2-4).

Fig. 3: Spectra for different angles θ_B. The curves labeled "averaged" have been calculated by integration over the solid angle assuming a Gaussian intensity profile for a cone of half angle 2°, centered at θ_B=90° (a) and θ_B=86° (b). The "averaged" shape is well approximated by an angle of 89° in (a), whereas for case (b) an integration is superfluous.

Fig. 4: Ion temperatures obtained by fitting "standard" (see table I) noiseless spectra with spectra calculated for incorrect density values.
Curve 1: freely adjustable intensity scale;
Curve 2: calibrated intensity scale.

Fig. 5: Ion temperatures obtained by fitting "standard" (see table I) noiseless spectra with spectra calculated for incorrect T_e values.
Curves are shown for 3 ion temperatures in D and for T_i = 400 eV in He.

Fig. 6: Ion temperatures obtained by fitting "standard" (see table I) noiseless spectra with spectra calculated for incorrect θ_B values. The corresponding curve for a "true" θ_B value of 86° is also shown.

Fig. 7: Ion temperatures obtained by fitting "standard" (see table I) noiseless spectra with spectra calculated for incorrect magnetic field values.

Fig. 8: Ion temperatures obtained by fitting "standard" (see table I) noiseless spectra with spectra calculated for incorrect impurity concentrations (curve 1), light impurities C and O only (curve 2) and heavy impurity Fe

only (curve 3). The "correct" Z_{eff} is always 2.53 and the relative impurity concentrations are kept fixed.

Fig. 9 Log of the least-squares-fitting merit function F plotted against T_i. In all cases the true T_i value is 400 eV.

(a) Noiseless "experimental" spectrum, plasma parameters n_e, T_e and B exactly and correctly known.

(b) Merit function for five simulated shots where "experimental" spectrum is noisy, but n_e, T_e, and B are exactly and correctly known. The fitted T_i-values are: 345, 406, 411, 446, 472 eV.

(c) Merit functions for five simulated shots where "experimental" spectrum is noisy , and n_e, T_e and B are only approximately known. The fitted T_i-values are: 146, 354, 357, 1166, 1541 eV.

Fig. 10 (a) Percentage shot-to-shot standard deviation,

(b) mean systematic percentage error in fitted T_i, both as function of fractional variation in given T_e.

Each point was obtained from 31 simulated shots. Values of all other parameters are as given in table 1.

Fig. 11 Fitted T_i as a function of the supplied value of T_e for about 300 simulated shots. The correct values of T_e and T_i are 700 eV and 400 eV respectively. Values of all other parameters are as given in table 1.

Fig. 12 (a) Percentage shot-to-shot standard deviation,

(b) mean systematic percentage error in fitted T_i, both as function of fractional variation in given impurity abundance.

Each point was obtained from 31 simulated shots. Values of all other parameters are as given in table 1.

Fig. 13 Fitted T_i as a function of the supplied fractional abundance of deuterium ions, for about 210 shots. The true values of D and T_i are 0.968 and 400 eV respectively.

Values of all other parameters are as given in table 1.

Fig. 14 Percentage shot-to shot standard deviation in fitted T_i as a function of "true T_i". Each point was obtained from 31 simulated shots.
Values of all other parameters are as given in table 1.

Fig. 15 Scattered spectra. The circles represent the signal recorded in each channel for a typical single simulated shot. The vertical bars give ± 1 standard deviation obtained from 31 such shots, and the solid line is the noiseless spectrum calculated from standard conditions given in table 1.

Fig. 16 (a) Percentage shot-to-shot standard deviation,
(b) mean systematic percentage error in fitted T_i, both as function of receiver NEP.
Each point was obtained from 31 simulated shots. Values of all other parameters are as given in table 1.

Fig. 17 (a) Percentage shot-to-shot standard deviation,
(b) mean systematic percentage error in fitted T_i, both as function of lower cutoff frequency of the first receiver channel.
Each point was obtained from 31 simulated shots. Values of all other parameters are as given in table 1.

Table I. **Standard input data set for a D-plasma.**

Subject	*Parameter*	*Symbol*	*Value*
Plasma	electron density	n_e	8.10^{13} cm^{-3}
	electron temperature	T_e	700 eV
	magnetic field	B	1.5 Tesla
	true ion temperature	T_{i0}	400 eV
	fractional abundance of the ion species :		
	Deuterium		0.968
	Carbon		0.02
	Oxygen		0.01
	Iron		0.002
	mass (in amu):		
	Deuterium		2.0
	Carbon		12.0
	Oxygen		16.0
	Iron		55.8
	charge (in electron charge units) :		
	Deuterium		1
	Carbon		6
	Oxygen		8
	Iron		19
	temperature : (for all impurity species)	T_{imp}	400 eV
	uncertainties expressed in standard deviations (SD) :		
	SD for n_e	Δn_e	0 (0.05)*
	SD for T_e	ΔT_e	0 (0.10)*
	SD for B	ΔB	0 (0.03)*
	SD for impurity abundance	ΔF_i	0 (0.4)*
	SD for impurity ion temp.	ΔT_{imp}	0
Scattering experiment	scattering angle	θ	90°
	angle to magnetic field**	θ_B	88°
	f number (focusing and detection optics)	f	13.5
Laser	wavelength	λ	385μm
	power	P	1.0 MW
	pulse duration	τ	1.38 μs
Receiver	noise equivalent power	NEP	$5{\cdot}10^{-19}$ W/Hz
	minimum IF frequency	ν_0	280 MHz ***
	channel width	$\Delta\nu$	80 MHz
	number of channels	N	12

Derived+	diameter of scattering volume	D_V	6.6 mm
	scattering parameter	α	1.97
	Debye length	λ_D	22 μm
	effective charge	Z_{eff}	2.53

* The values in brackets are estimated for typical TCA tokamak conditions.

** θ_B is the angle between the scattering k-vector and the magnetic field B.

*** The zero of the IF-scale corresponds to the D_2O laser line and hence the centre of the spectrum. The first IF-channel covers the band from 280 to 360 MHz.

\+ These values are calculated from the input parameters.

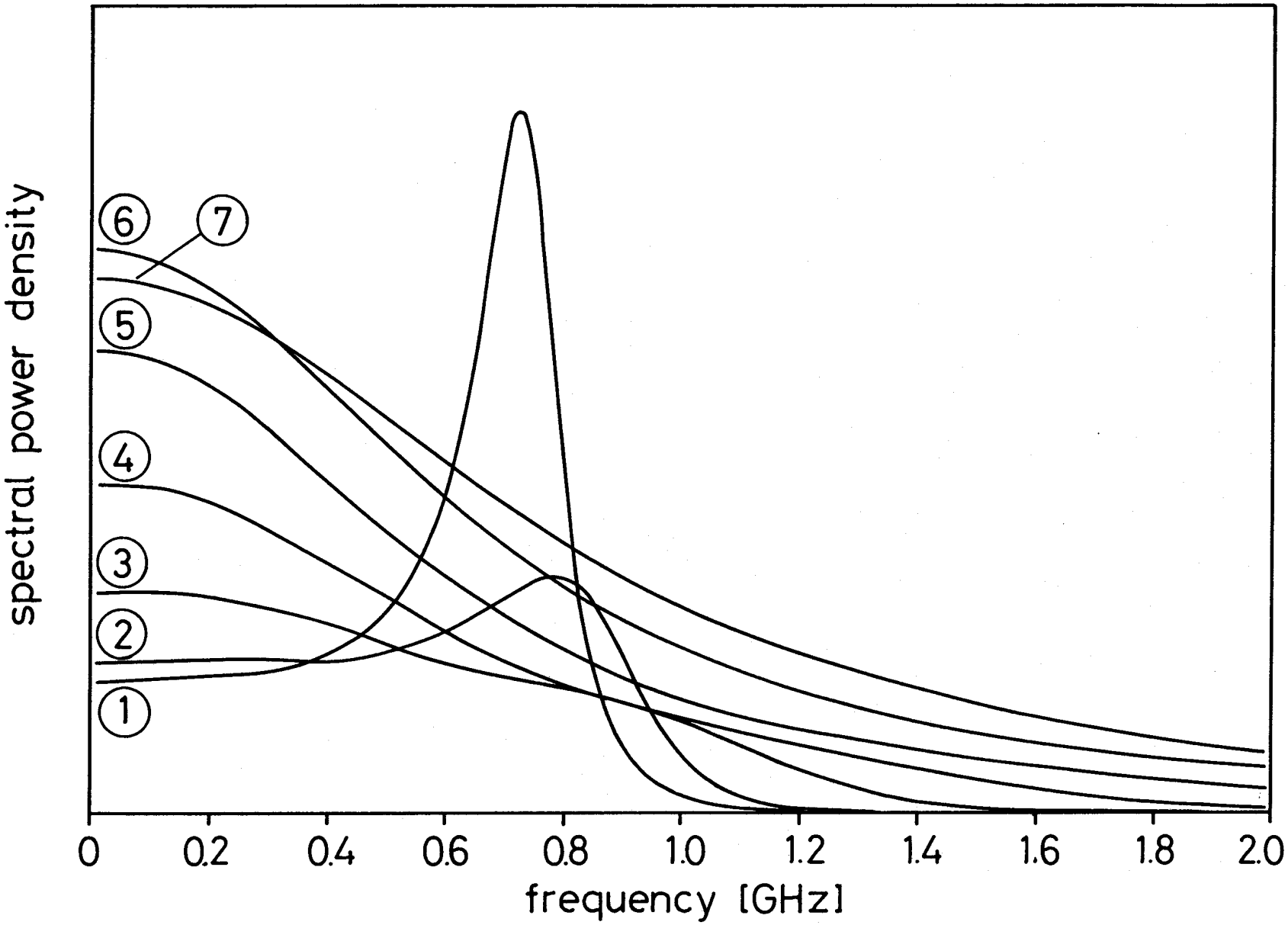
spectral power density
6
7
5
4
3
2
1
0
0.2
0.4
0.6
0.8
1.0
1.2
1.4
1.6
1.8
2.0
frequency [GHz]

FIG. 1

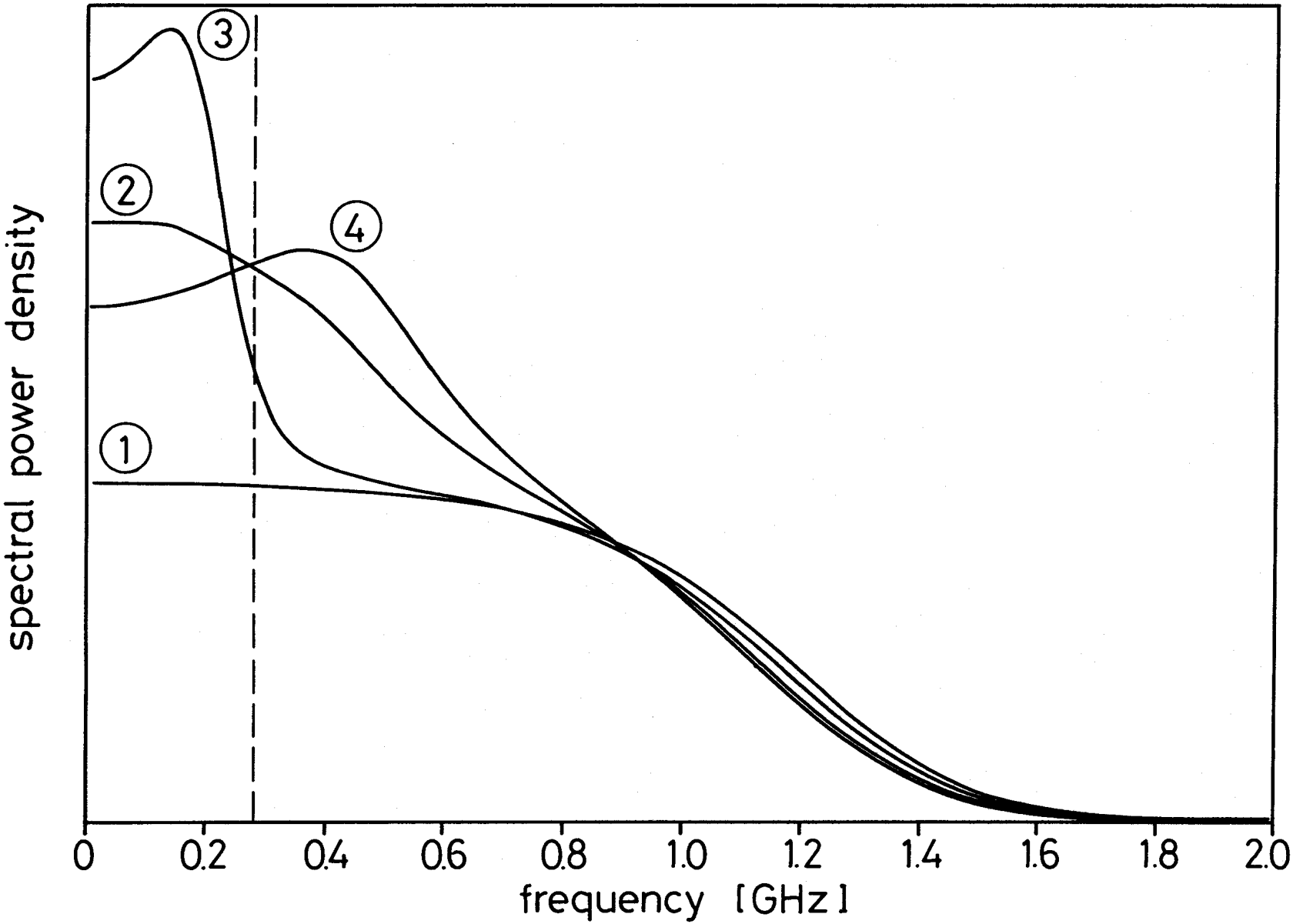
spectral power density
3
2
4
1
0
0.2
0.4
0.6
0.8
1.0
1.2
1.4
1.6
1.8
2.0
frequency [GHz]

FIG. 2

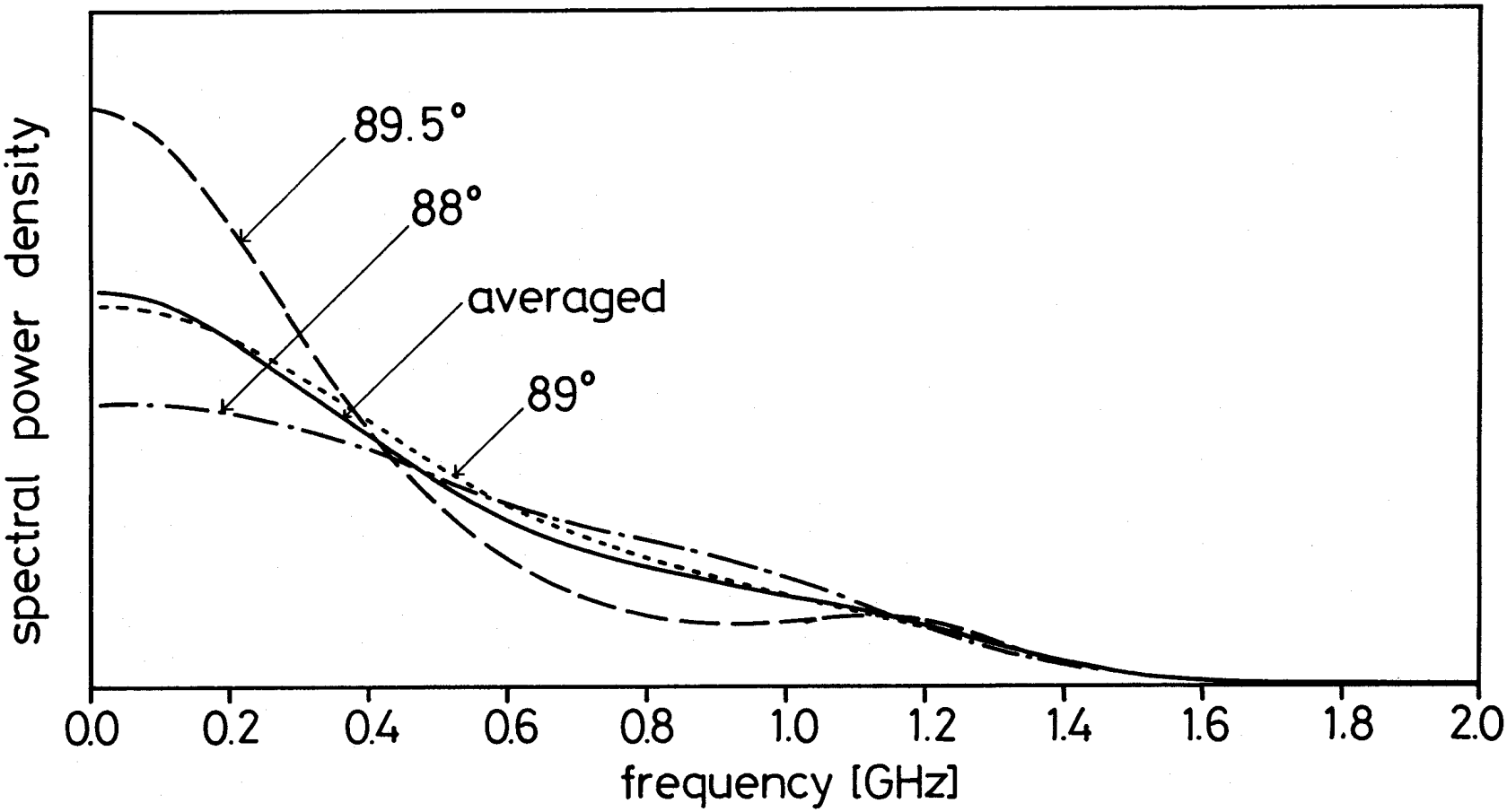
spectral power density
89.5°
88°
averaged
89°
0.0
0.2
0.4
0.6
0.8
1.0
1.2
1.4
1.6
1.8
2.0
frequency [GHz]

FIG. 3 A

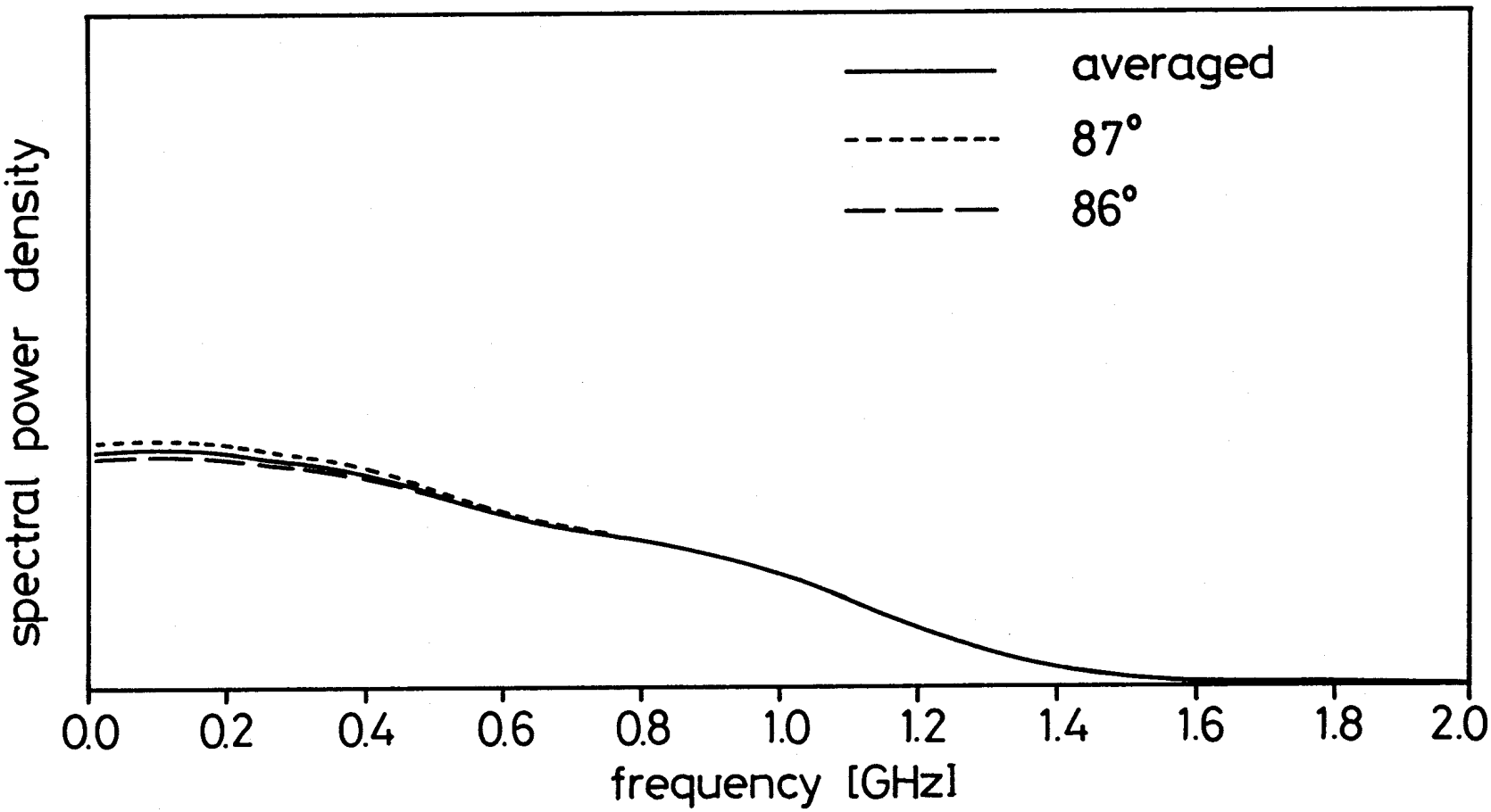
averaged
87°
86°
spectral power density
0.0
0.2
0.4
0.6
0.8
1.0
1.2
1.4
1.6
1.8
2.0
frequency [GHz]

FIG. 3B

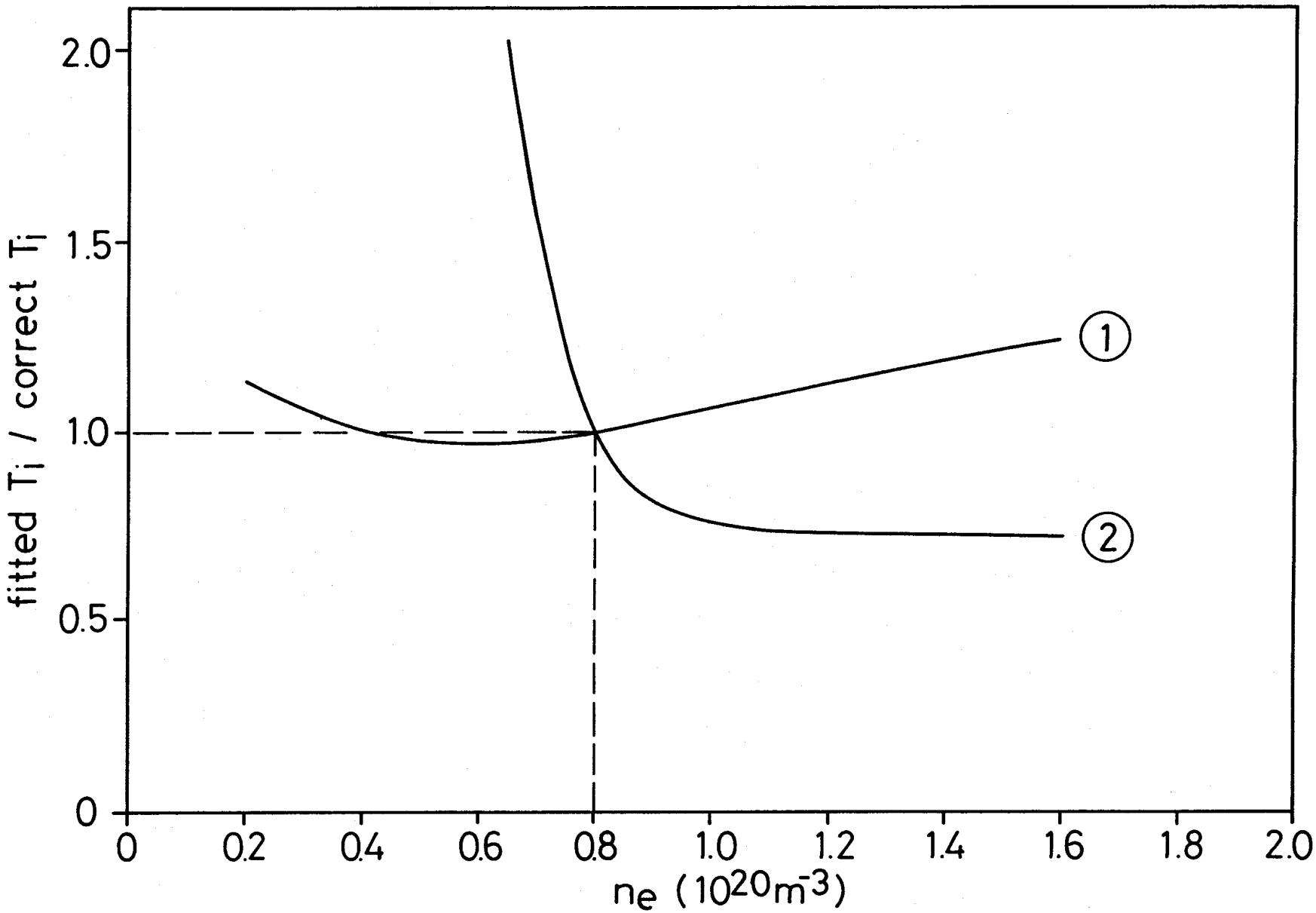
2.0
1.5
1.0
0.5
0
fitted T_i / correct T_i
0
0.2
0.4
0.6
0.8
1.0
1.2
1.4
1.6
1.8
2.0
n_e ($10^{20}m^{-3}$)
1
2

FIG. 4

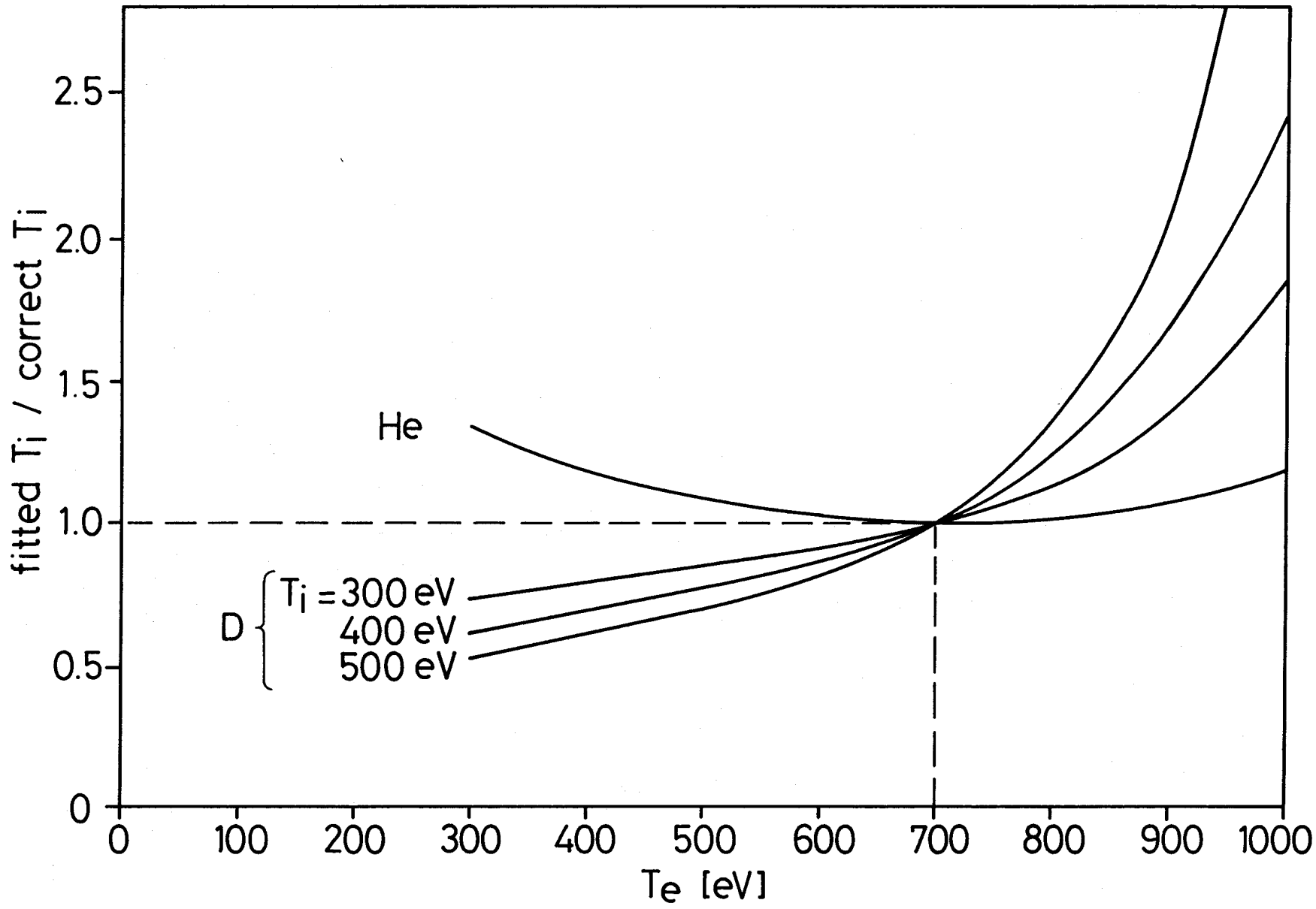
fitted Ti / correct Ti
2.5
2.0
1.5
1.0
0.5
0
He
D
Ti = 300 eV
400 eV
500 eV
0
100
200
300
400
500
600
700
800
900
1000
Te [eV]

FIG. 5

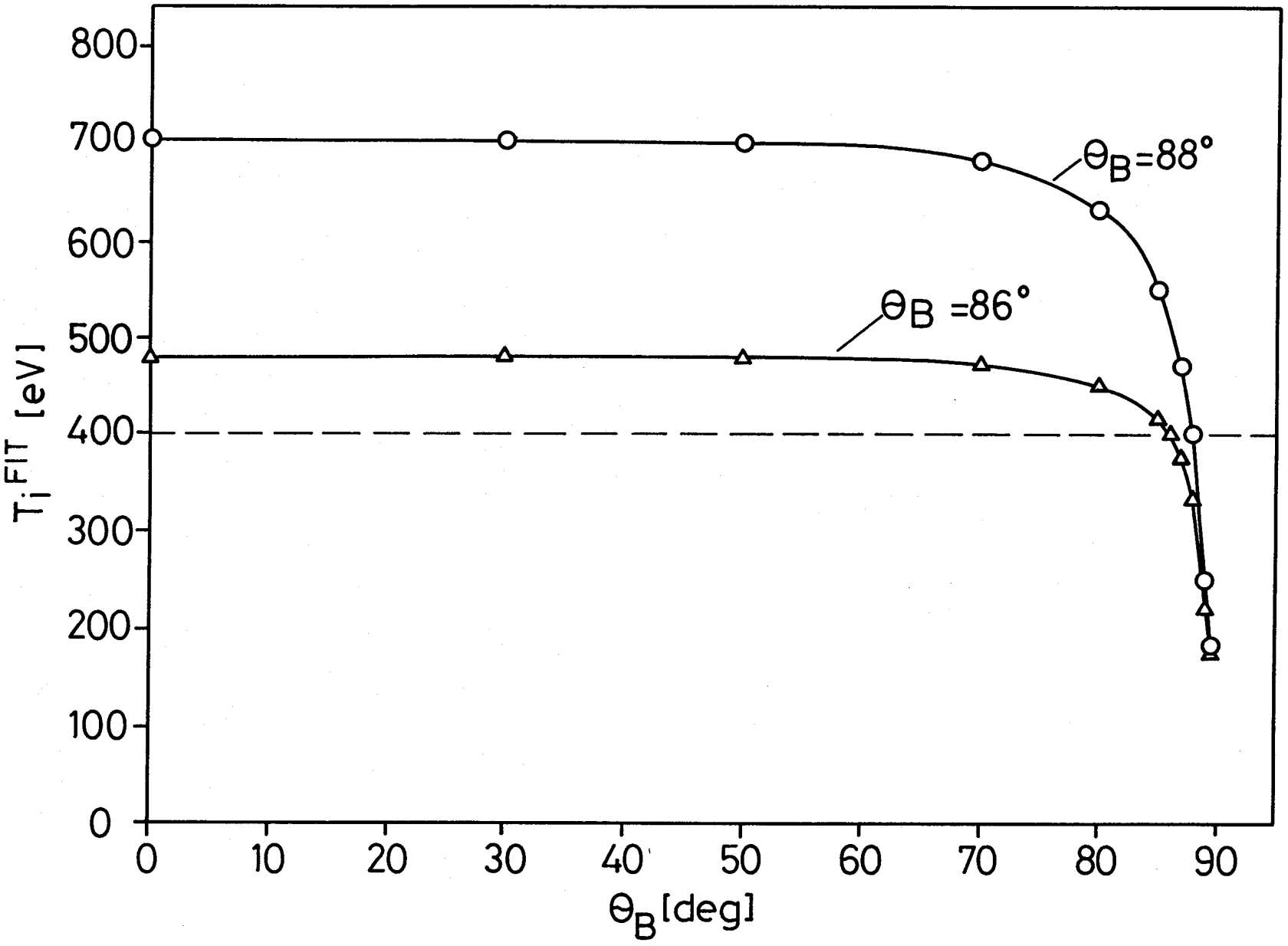
800
700
600
500
400
300
200
100
0
T_i^{FIT} [eV]
0
10
20
30
40
50
60
70
80
90
Θ_B [deg]
Θ_B=88°
Θ_B =86°

FIG. 6

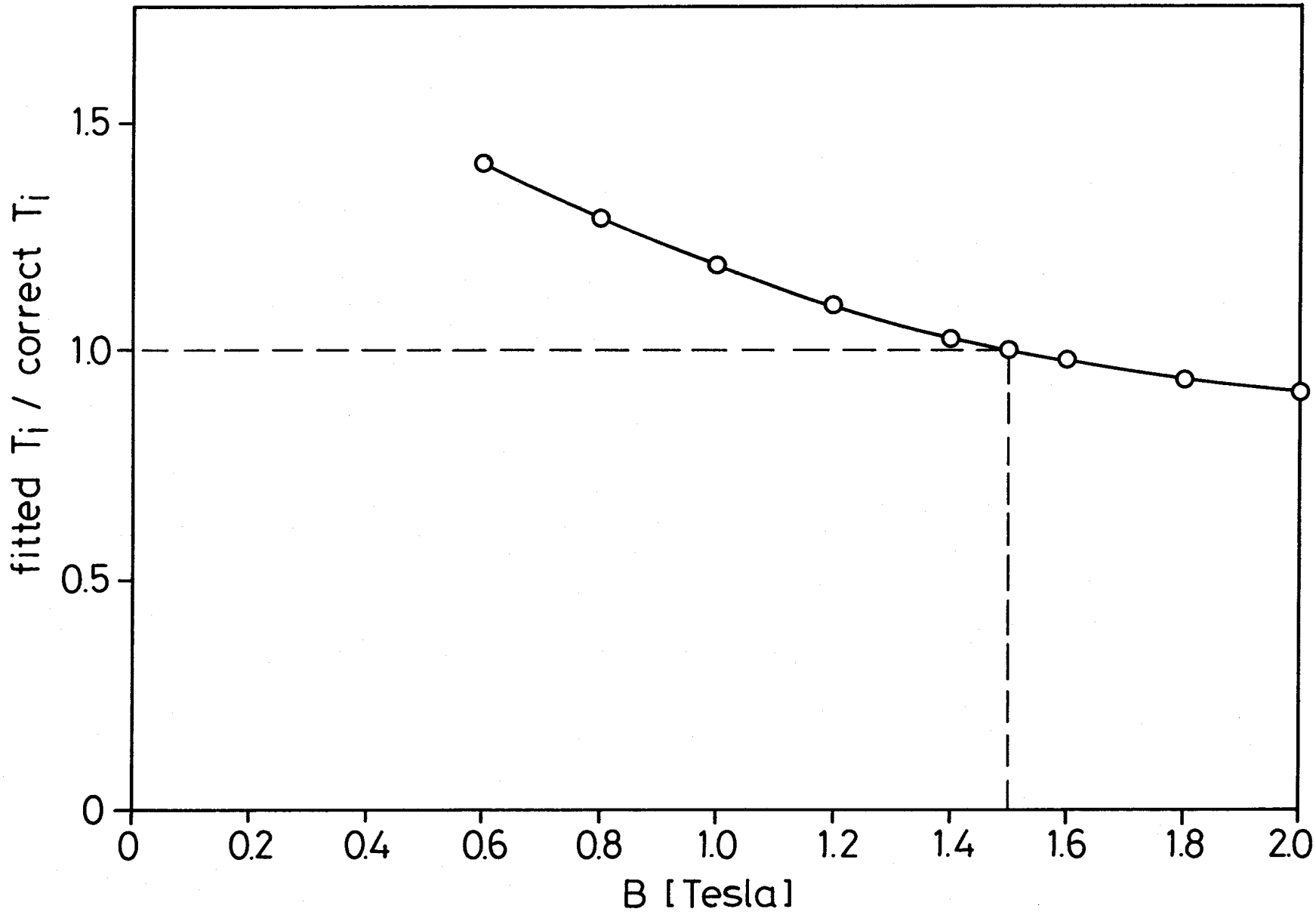
fitted T_i / correct T_i
1.5
1.0
0.5
0
0
0.2
0.4
0.6
0.8
1.0
1.2
1.4
1.6
1.8
2.0
B [Tesla]

FIG. 7

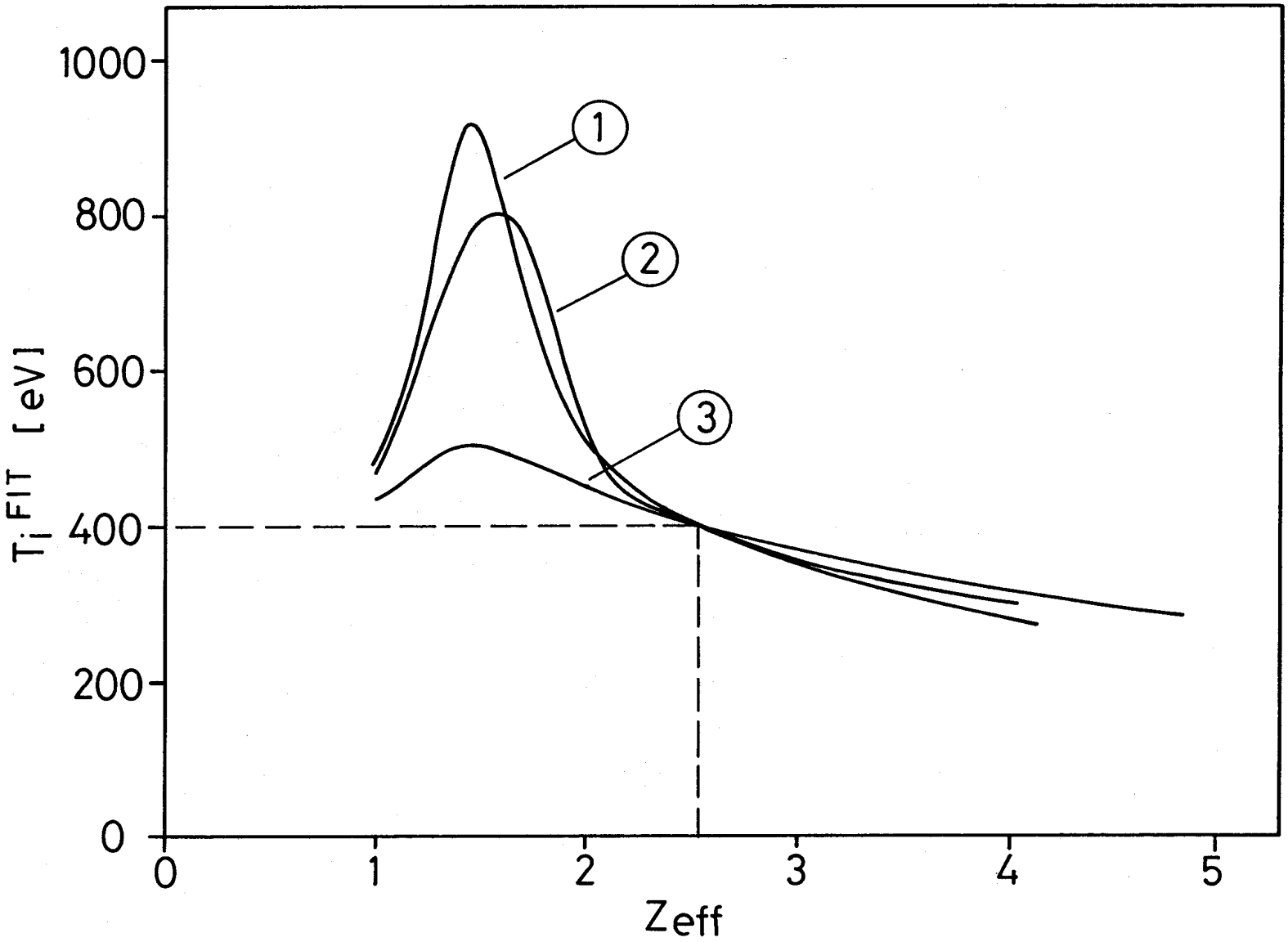

FIG. 8

FIG. 9

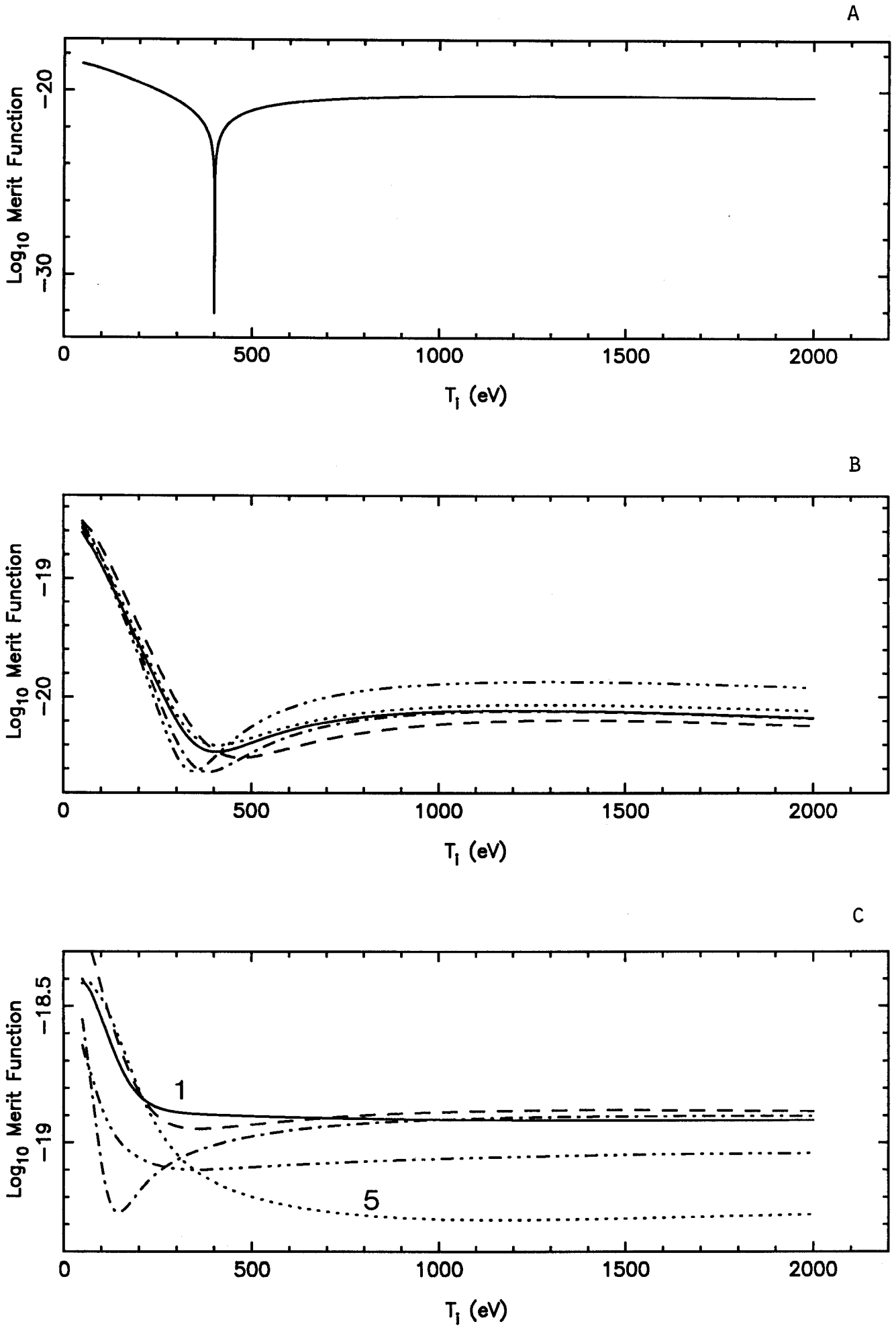
A
Log10 Merit Function
-20
-30
0
500
1000
1500
2000
Ti (eV)
B
Log10 Merit Function
-19
-20
0
500
1000
1500
2000
Ti (eV)
C
Log10 Merit Function
-18.5
-19
1
5
0
500
1000
1500
2000
Ti (eV)

FIG. 10

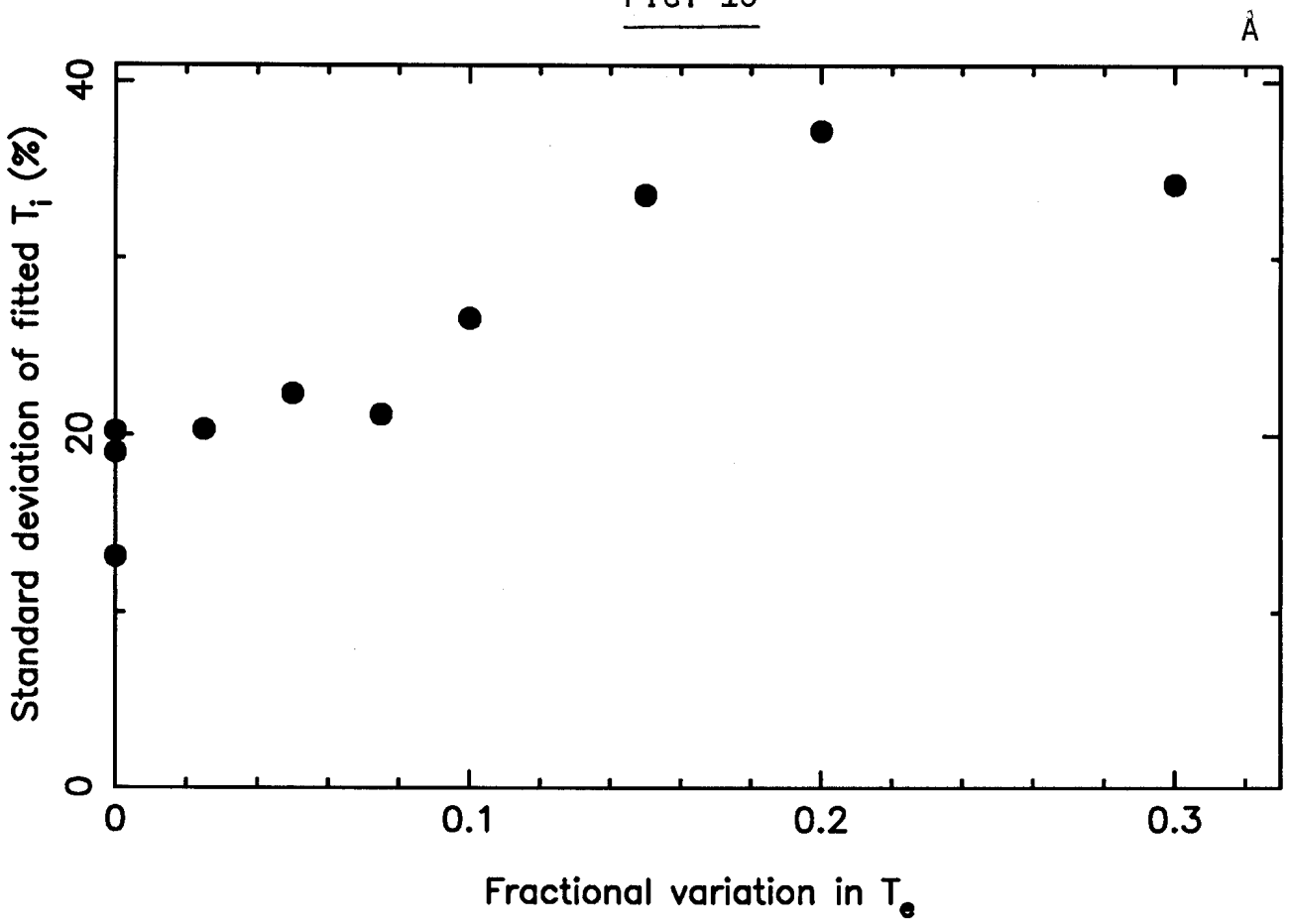
A
Standard deviation of fitted T_i (%)
0
20
40
0
0.1
0.2
0.3
Fractional variation in T_e

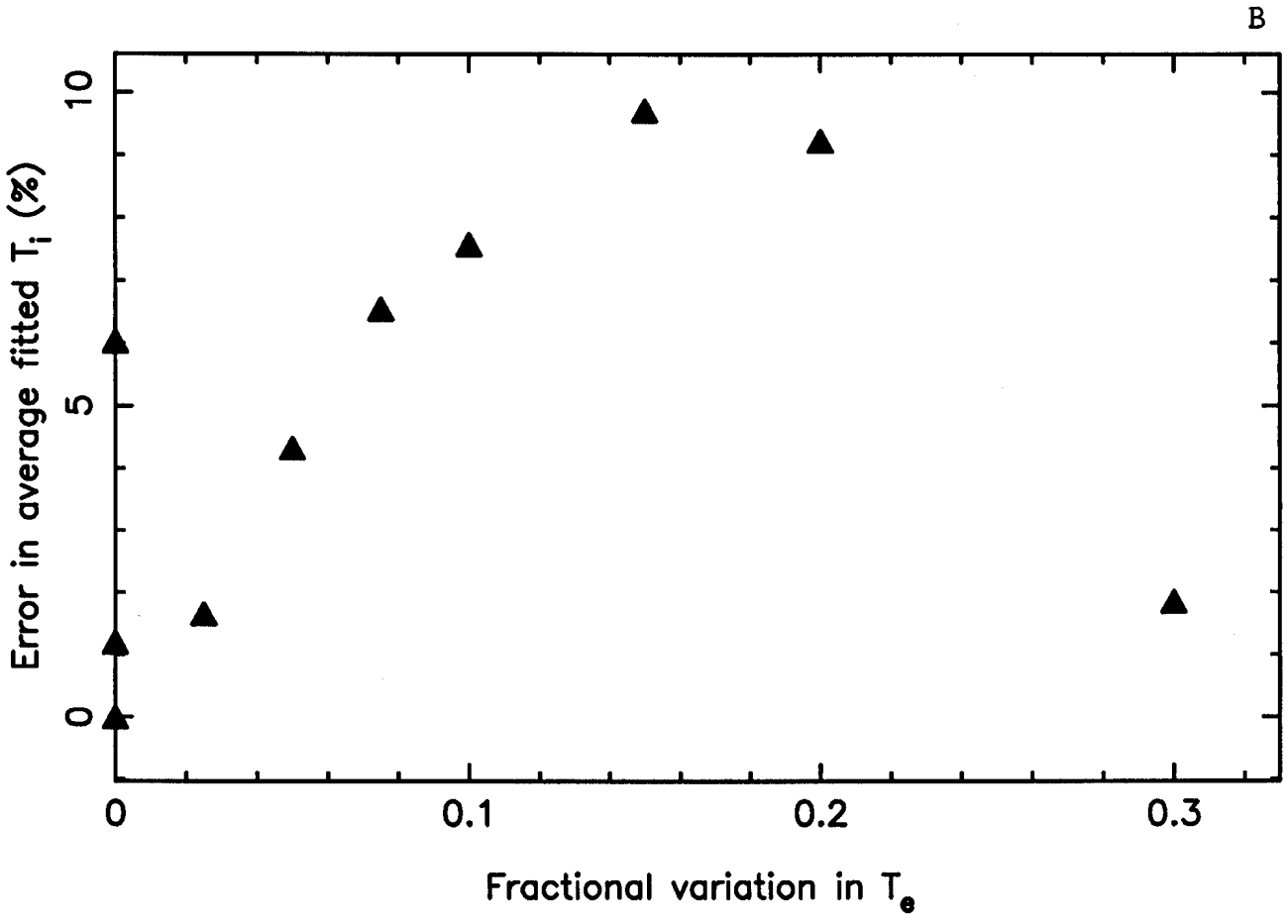
B
Error in average fitted T_i (%)
0
5
10
0
0.1
0.2
0.3
Fractional variation in T_e

FIG. 11

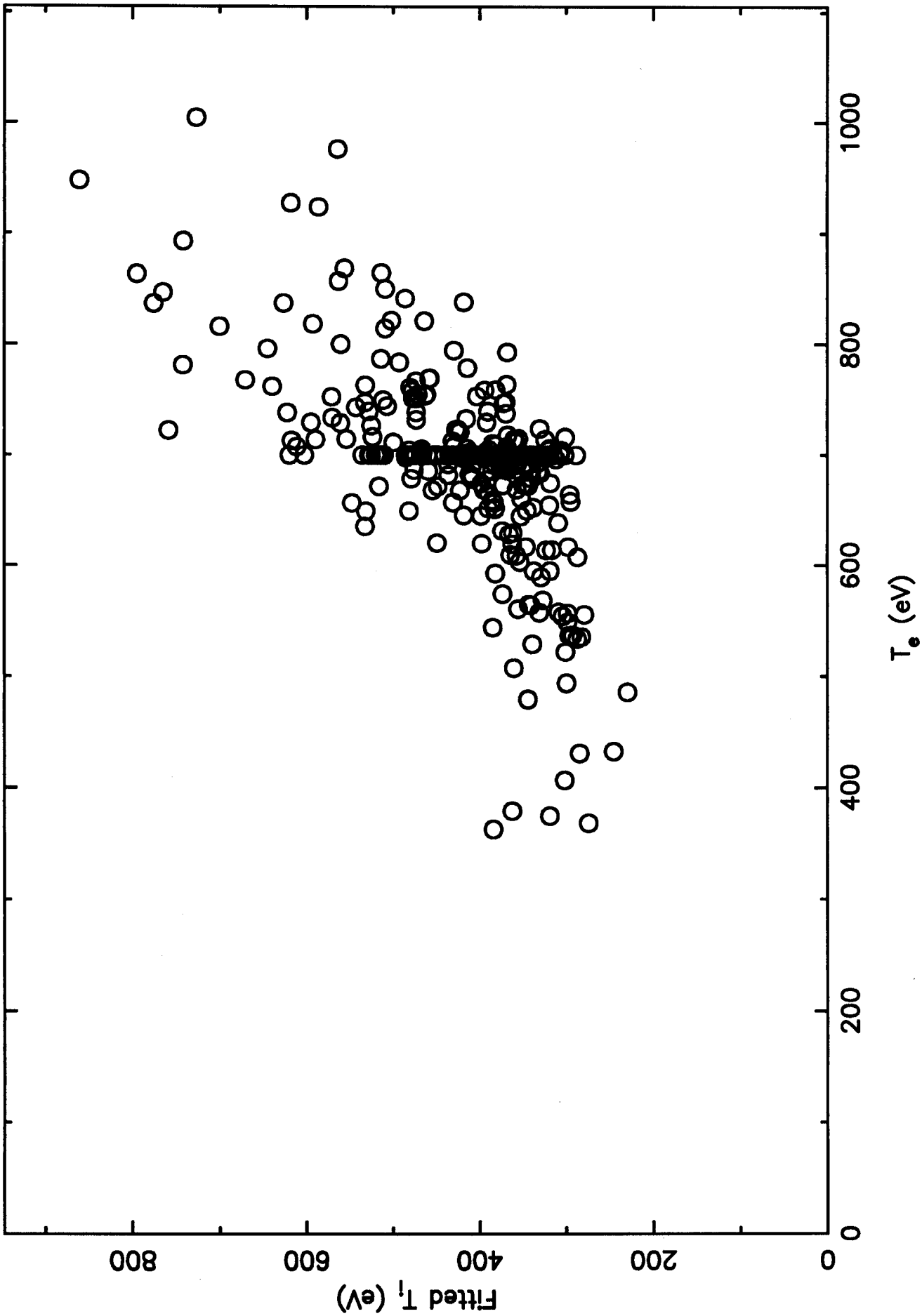

FIG. 12

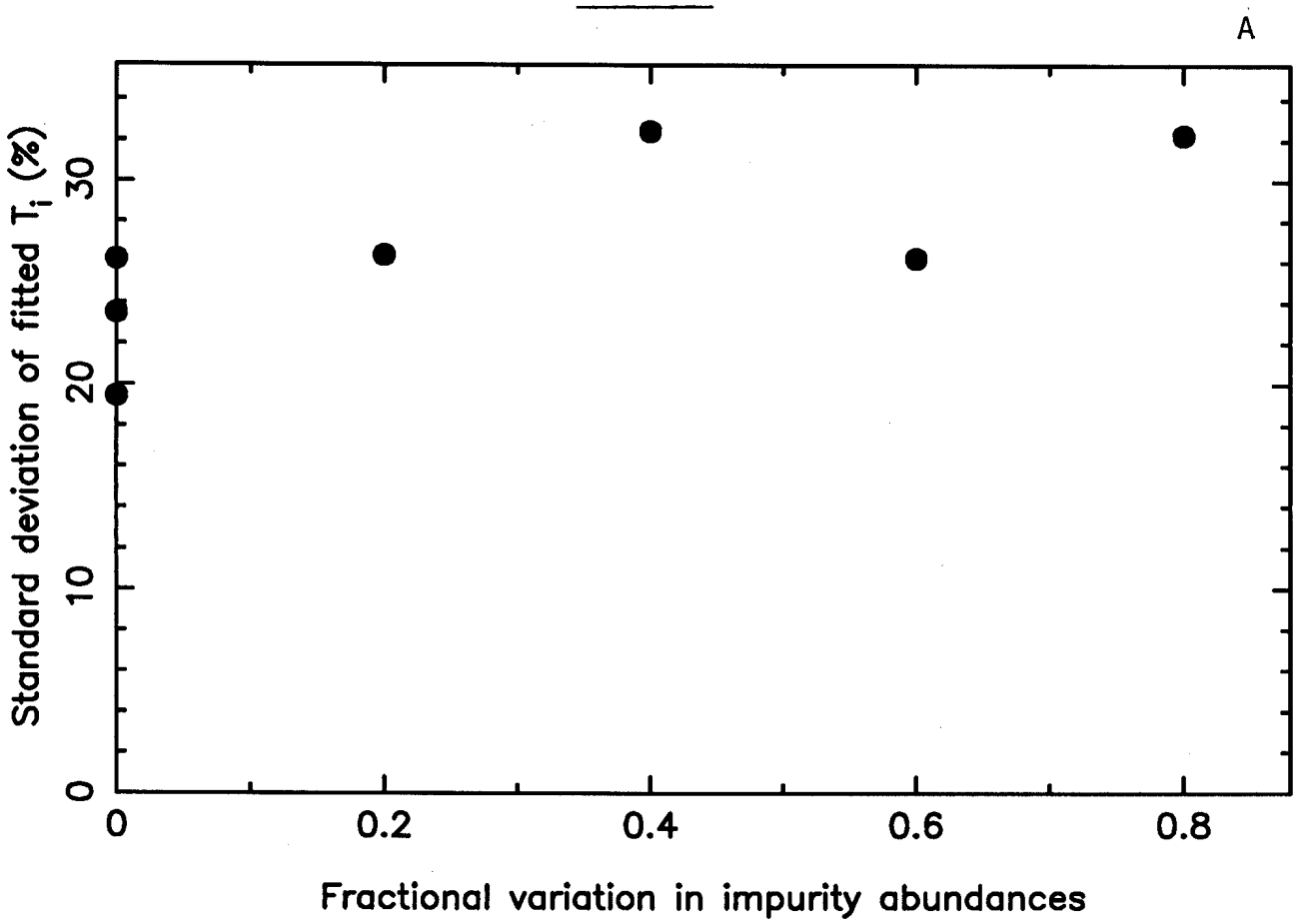
A
Standard deviation of fitted T_i (%)
0
10
20
30
0
0.2
0.4
0.6
0.8
Fractional variation in impurity abundances

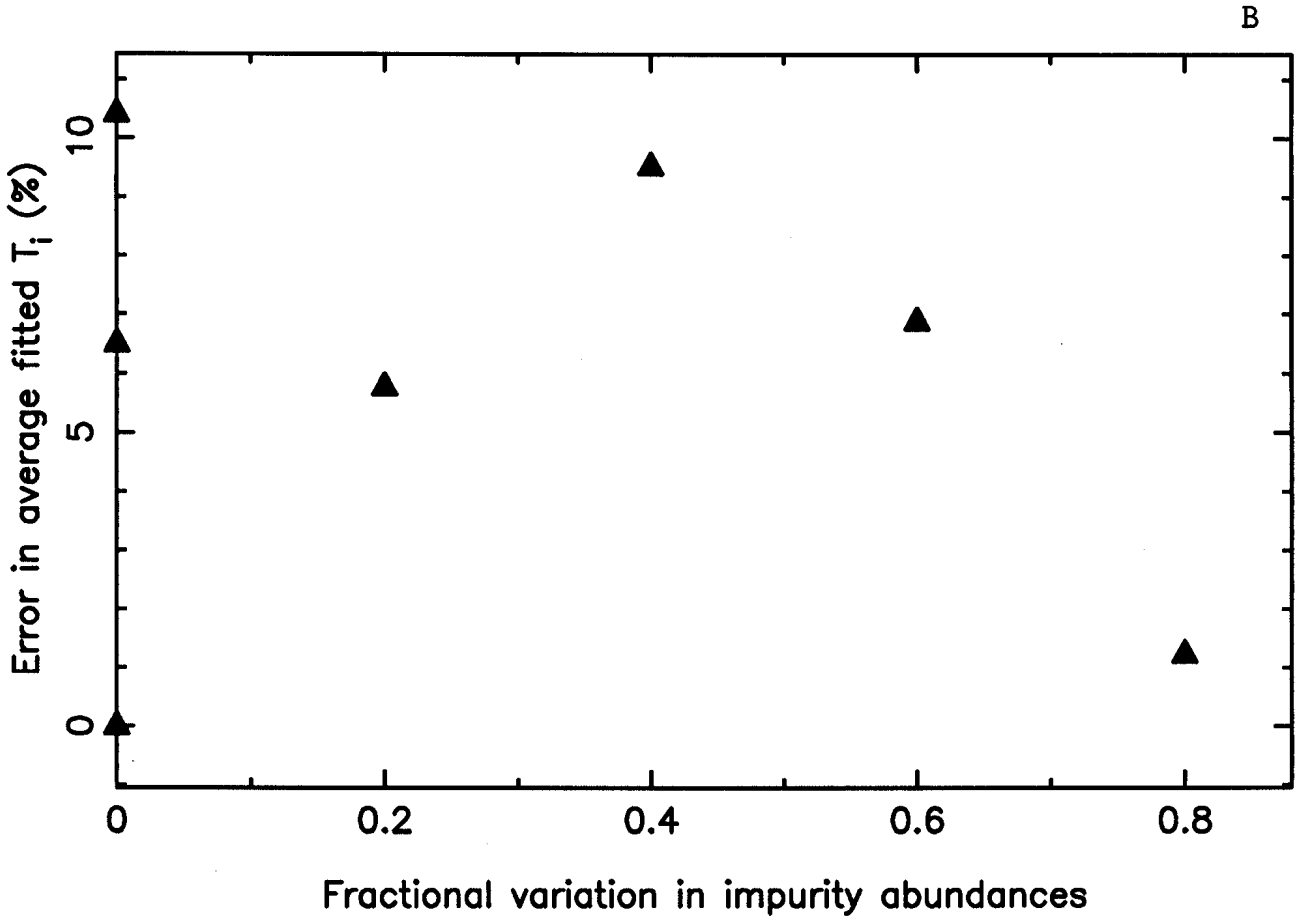
B
Error in average fitted T_i (%)
0
5
10
0
0.2
0.4
0.6
0.8
Fractional variation in impurity abundances

FIG. 13

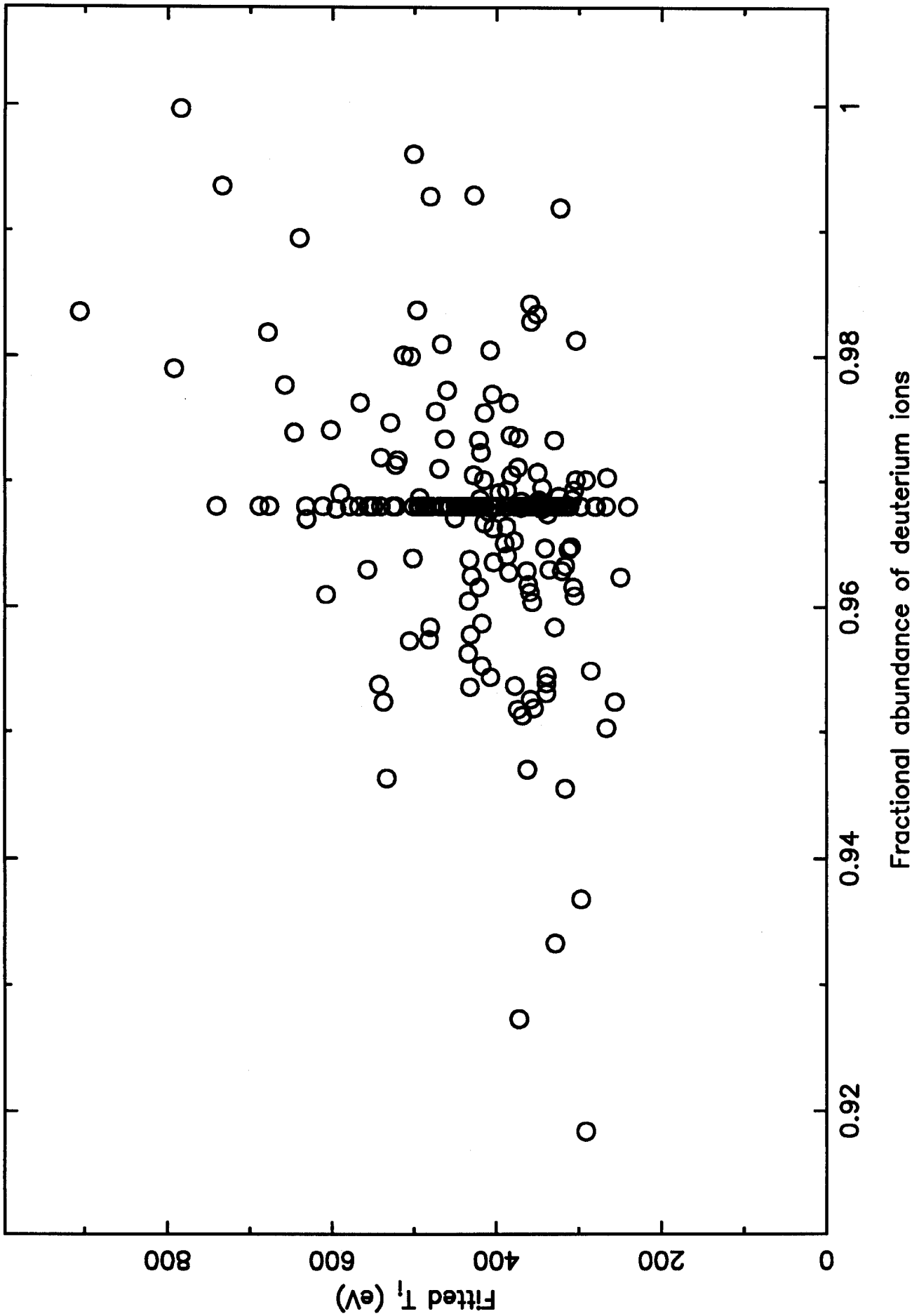
Fitted T_i (eV)
0
200
400
600
800
Fractional abundance of deuterium ions
0.92
0.94
0.96
0.98
1

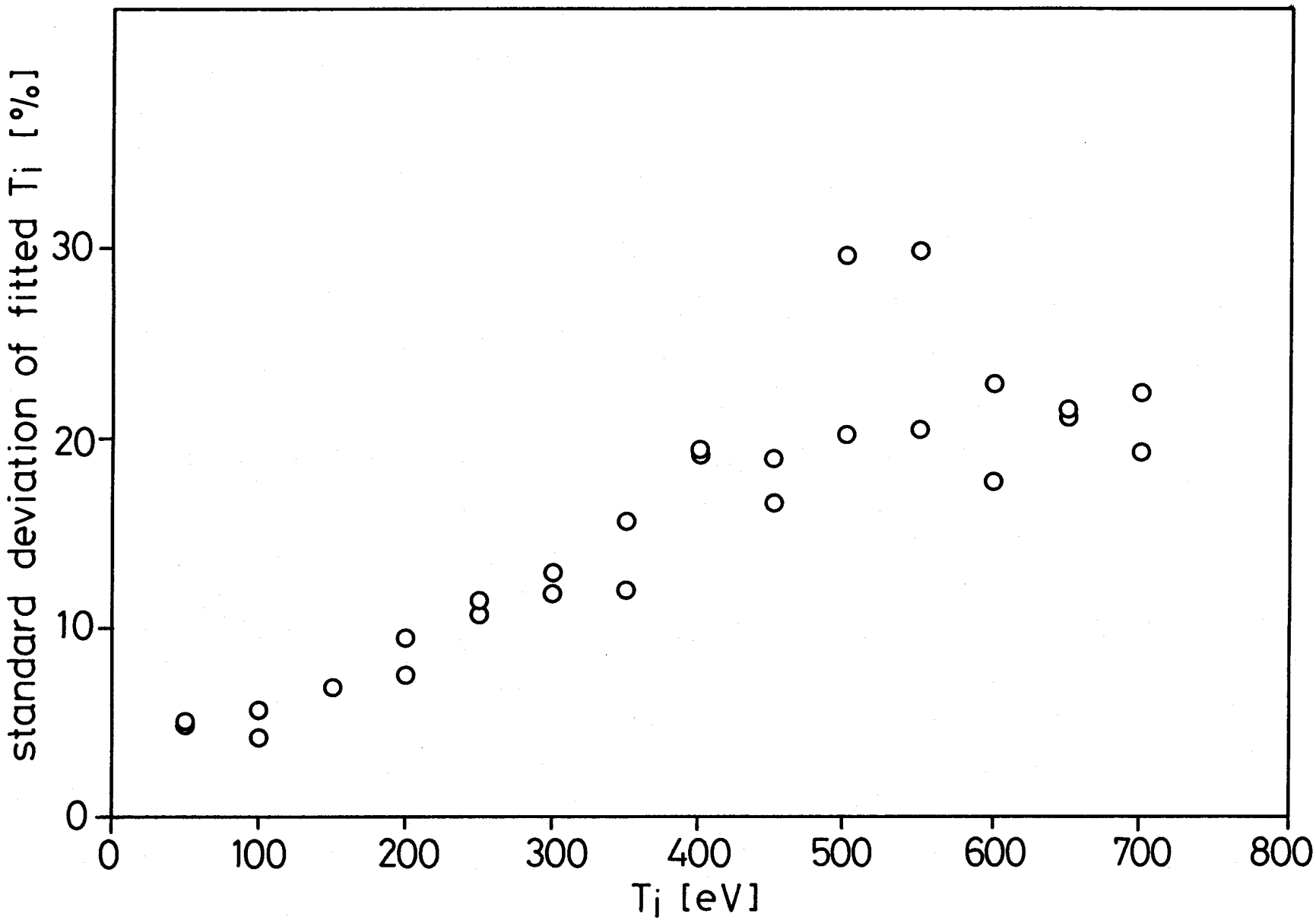
standard deviation of fitted Ti [%]
0
10
20
30
0
100
200
300
400
500
600
700
800
Ti [eV]

FIG. 14

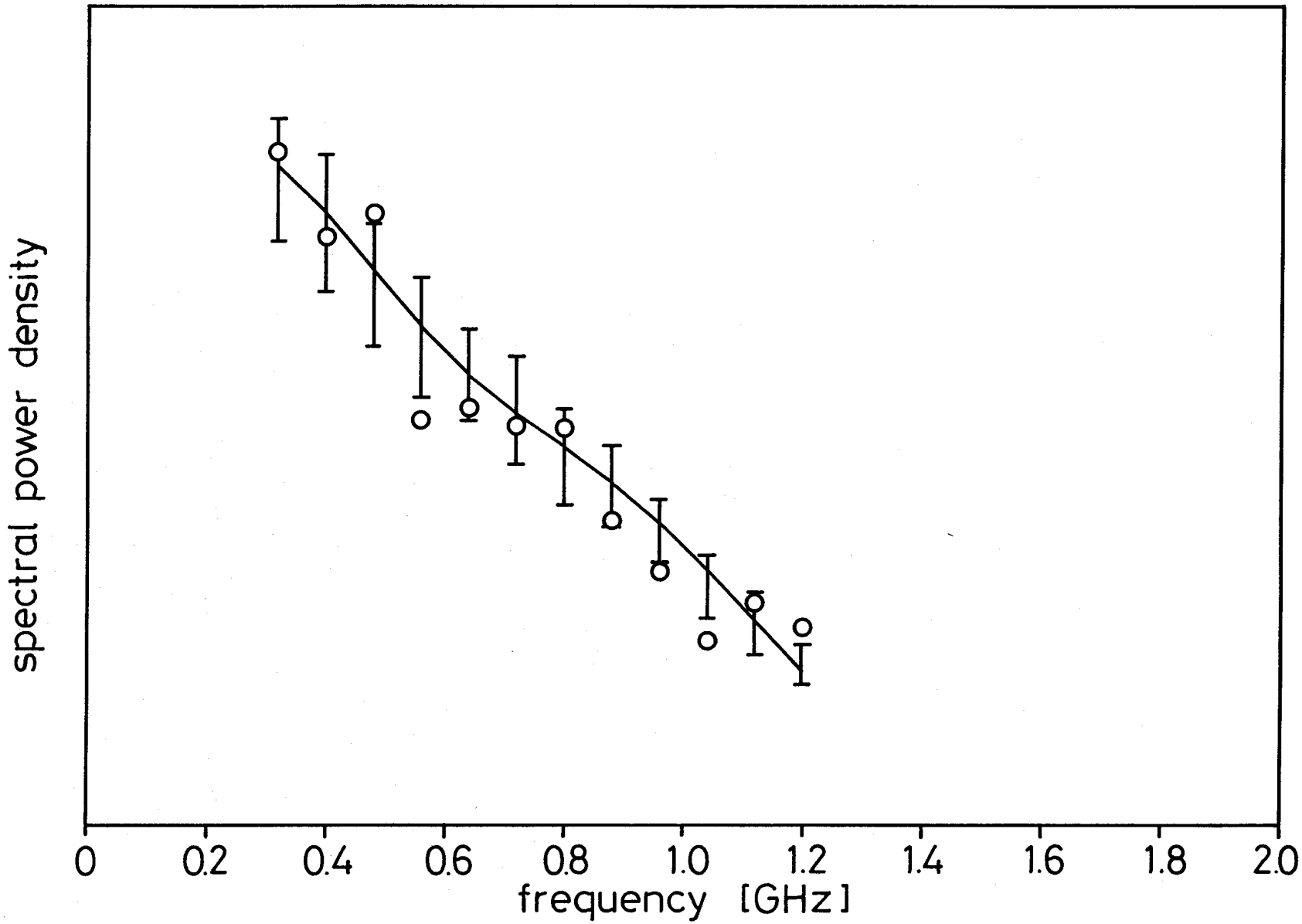
spectral power density
0
0.2
0.4
0.6
0.8
1.0
1.2
1.4
1.6
1.8
2.0
frequency [GHz]

FIG. 15

FIG. 16

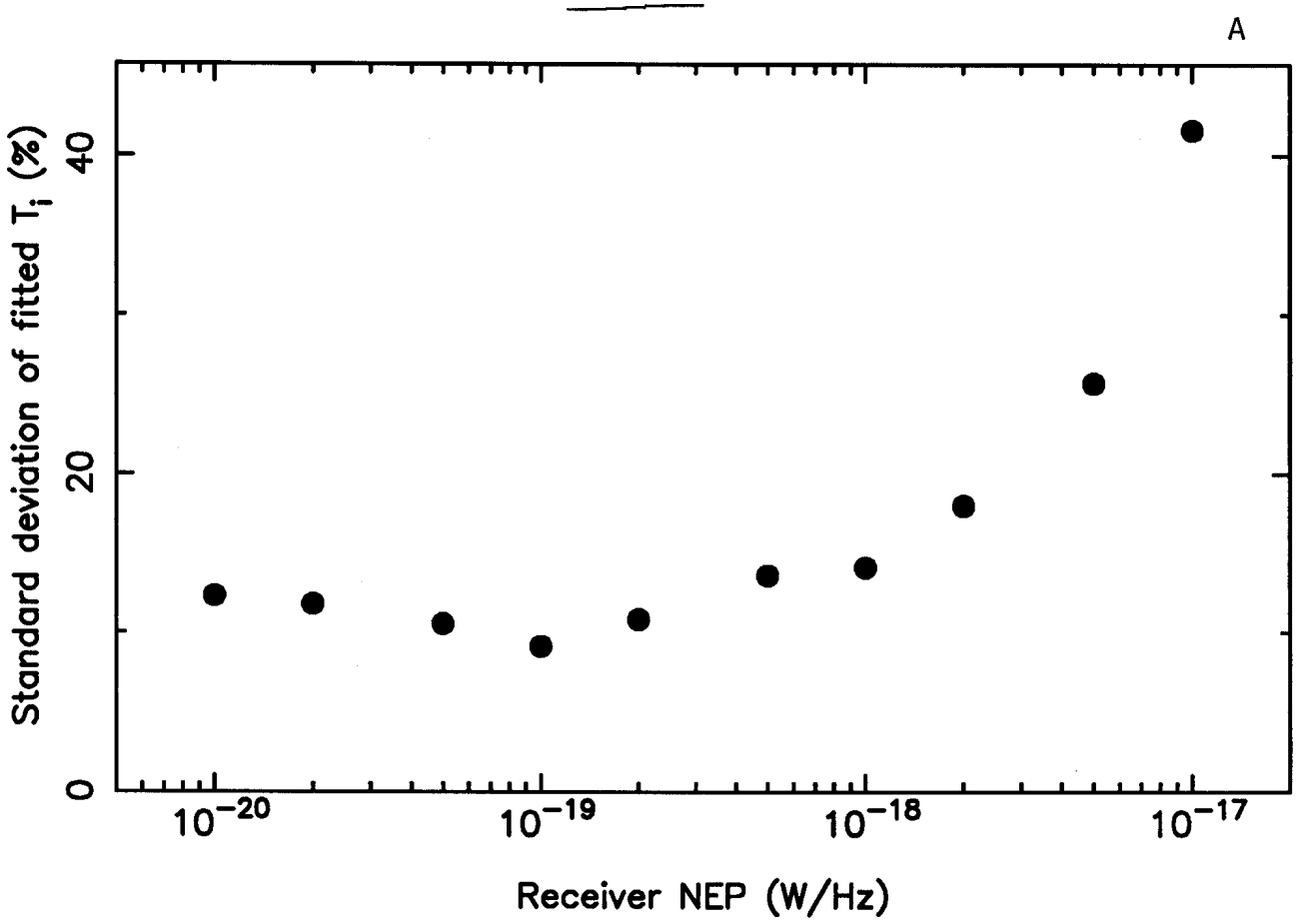
A
Standard deviation of fitted T_i (%)
0
20
40
10^{-20}
10^{-19}
10^{-18}
10^{-17}
Receiver NEP (W/Hz)

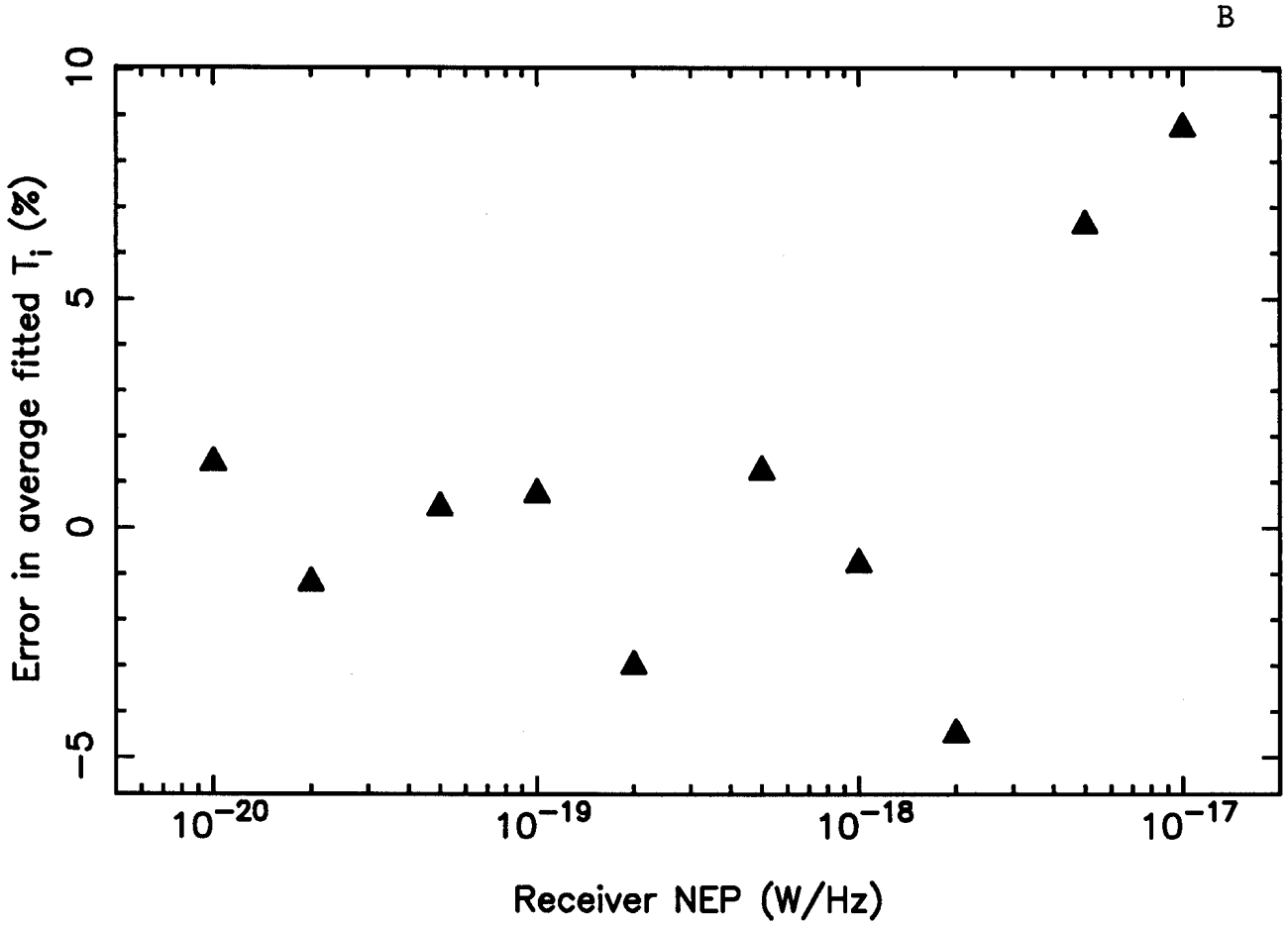
B
Error in average fitted T_i (%)
−5
0
5
10
10^{-20}
10^{-19}
10^{-18}
10^{-17}
Receiver NEP (W/Hz)

FIG. 17

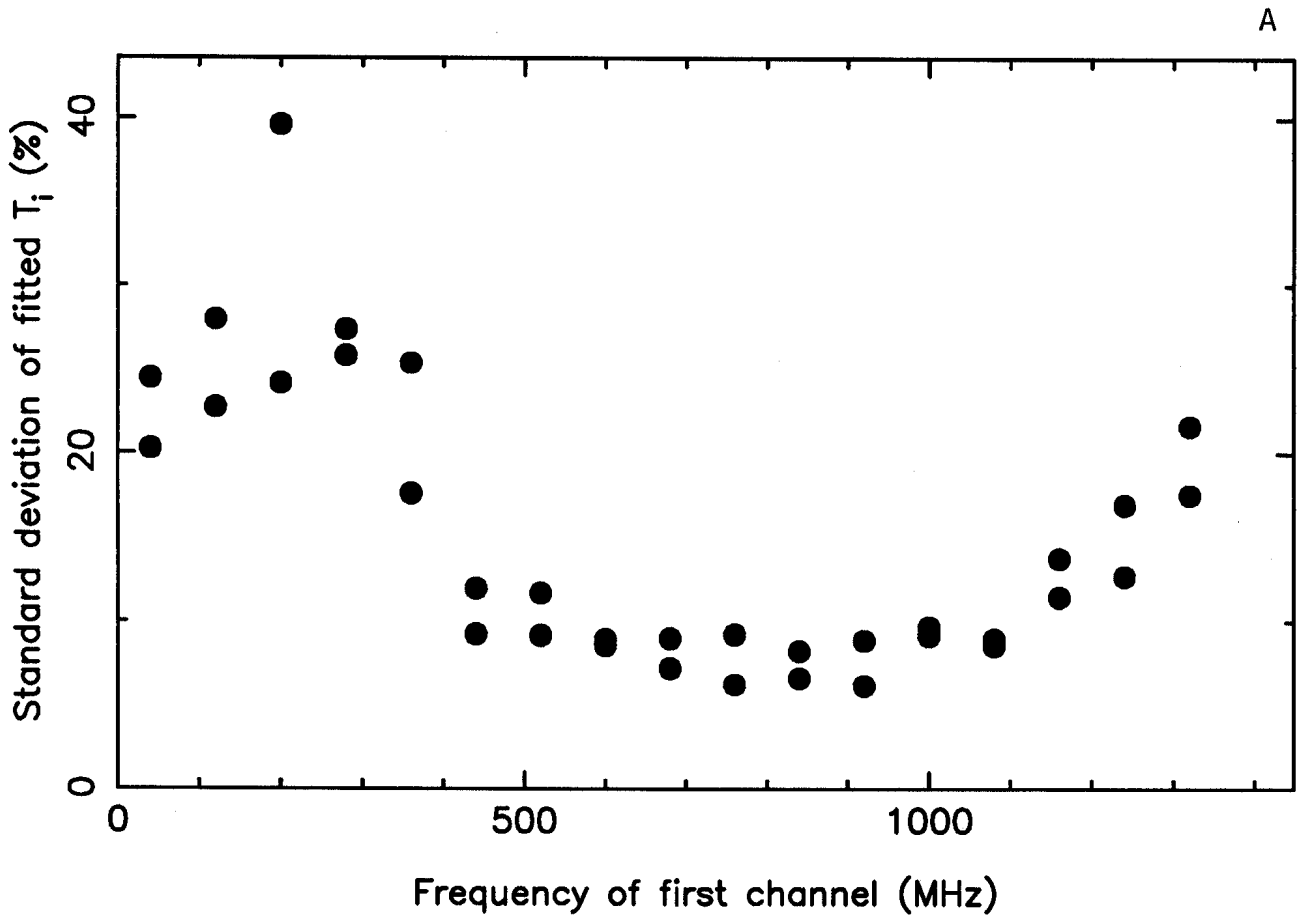
A
Standard deviation of fitted T_i (%)
0
20
40
0
500
1000
Frequency of first channel (MHz)

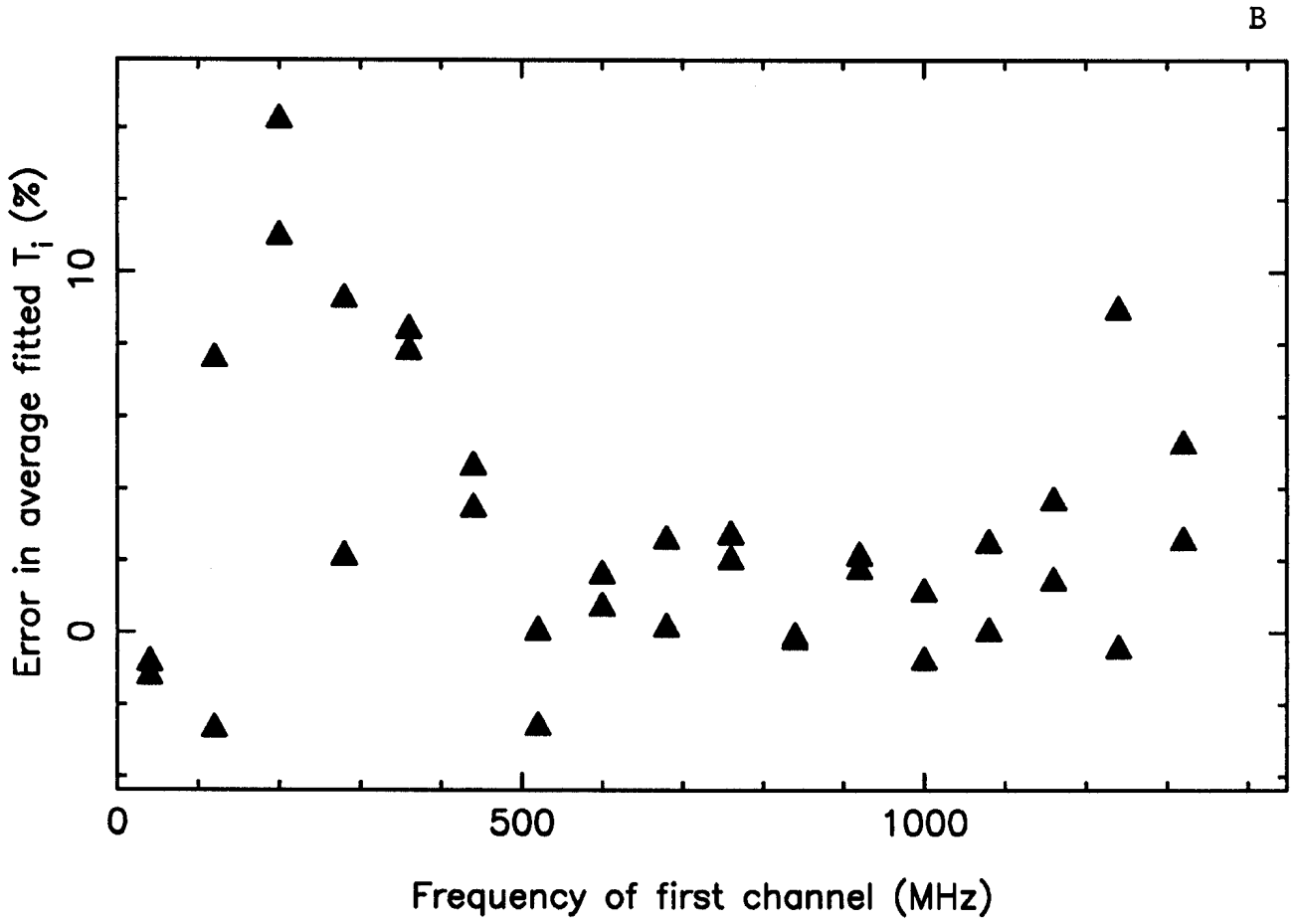
B
Error in average fitted T_i (%)
0
10
0
500
1000
Frequency of first channel (MHz)